Imaging Diagnostico e Tecnologie in TC

al di là dei "numeri"

Pisa, 20/12/2016

Vito Faranna

“stato dell’arte”

PUREViSION Optics

From photon generation, beam distribution to efficient detection

X-ray Generation

- Small focal spot utilization for a wider variety of exams

X-ray Beam Distribution

- Re-engineered Optics Assay for optimized X-ray beam spectrum

X-ray Transmission

- Adaptive scatter correction ensuring uniform image quality

X-ray Detection

- PUREViSION Detector – high precision manufacturing process produces a scintilator with 40% increased light output

X-Ray Beam Distribution

- Optimized X-Ray Beam Spectrum
  - Adaptive beam shaping optics ensure homogenous photon spread maximizing image resolution, while minimizing dose in a variety of clinical tasks
  - Reduction in low energy scattered radiation

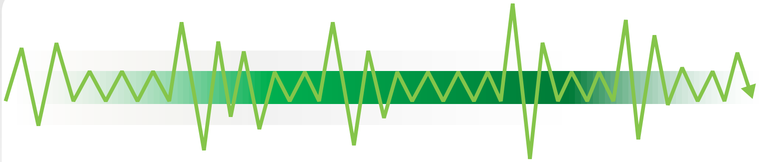

Old Beam Spectrum

New Beam Spectrum

TOSHIBA MEDICAL

X-Ray Transmission

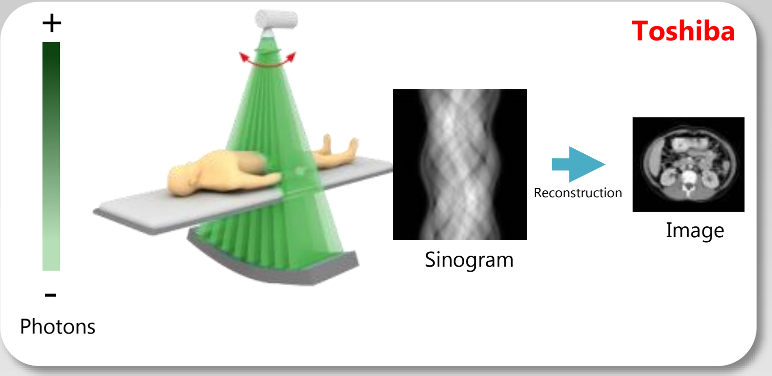

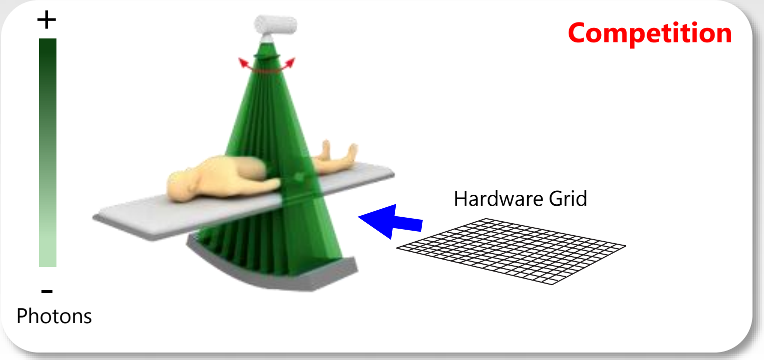

Two ways of managing scatter

Toshiba

- Adaptive scatter correction utilizing raw data based smart modeling ensures uniform image quality
- More primary photons are preserved for reconstruction = **EFFICIENCY**

Competitors utilize 3D hardware grid

- Primary photon absorption by the grid before detection
- Increase in exposure required to maintain signal to noise ratio

X-Ray Detection

Breakthrough manufacturing techniques

- **PUREViSION detector -** 40% increased light output resulting in higher detector efficiency

- Micro-blade cutting of a single ceramic ingot reduces imperfections ensuring superior luminescent properties

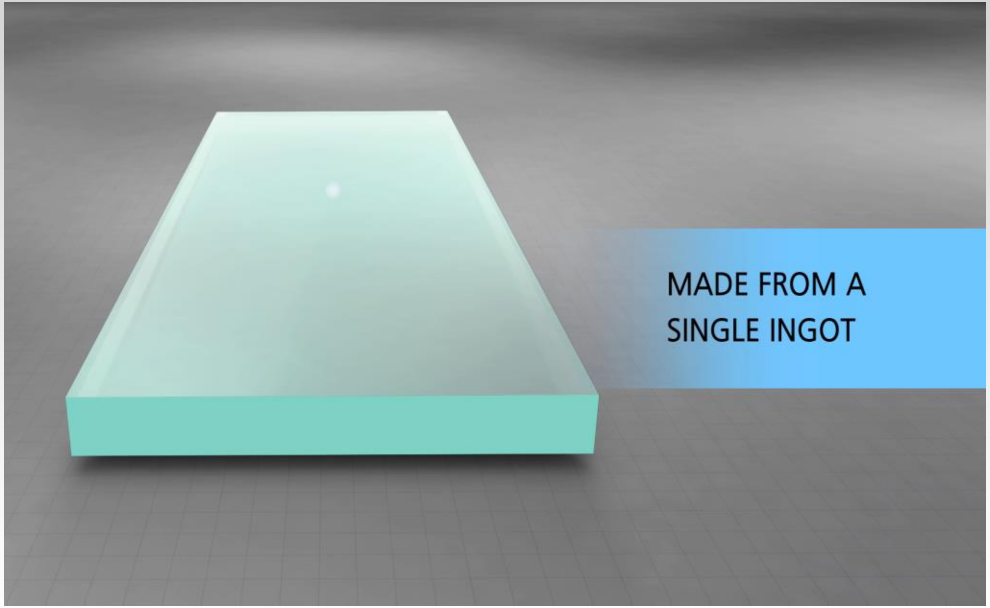

TOSHIBA MEDICAL

Physics

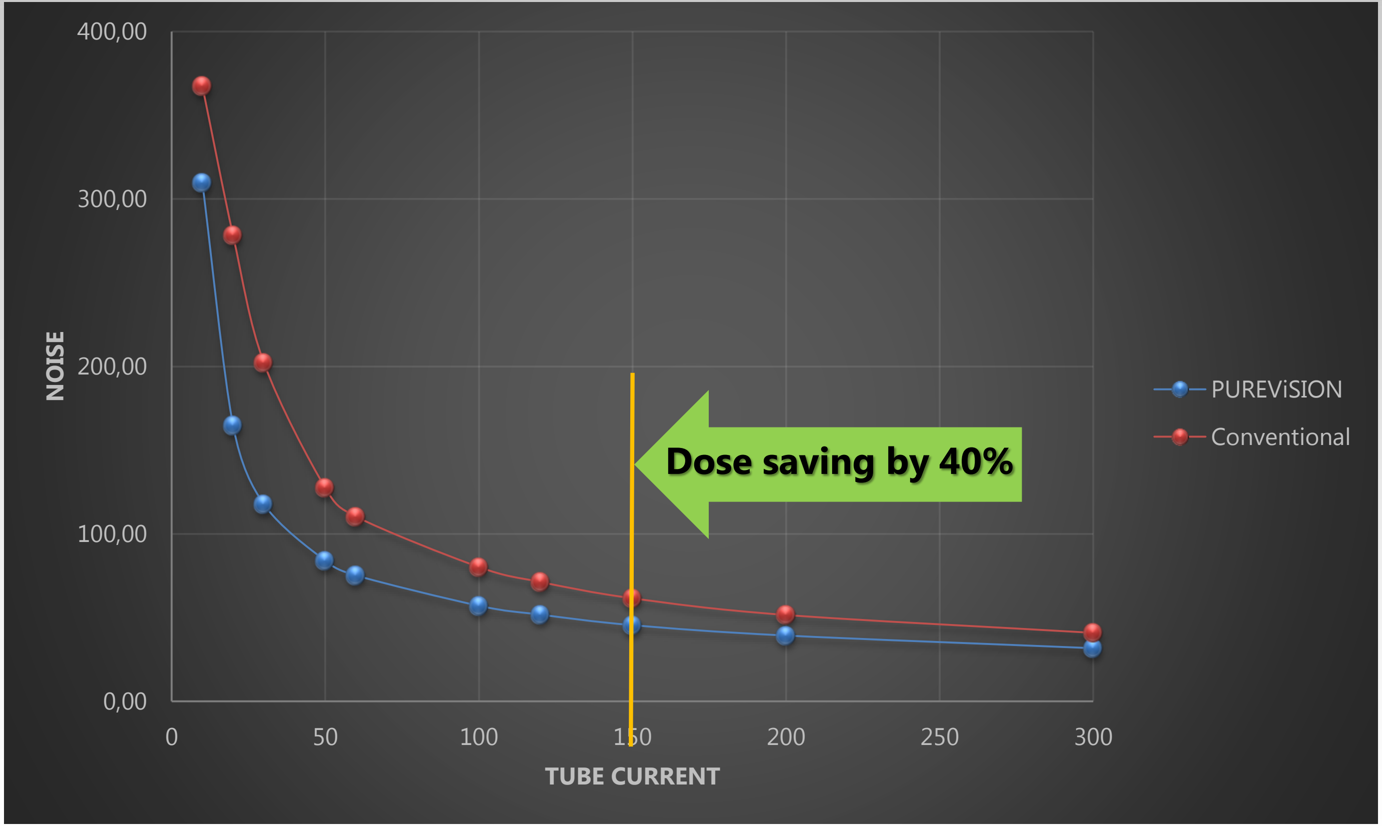

400,00
300,00
200,00
100,00
0,00
NOISE
0
50
100
150
200
250
300
TUBE CURRENT
Dose saving by 40%
PUREViSION
Conventional

Clinics (risparmio di MDC)

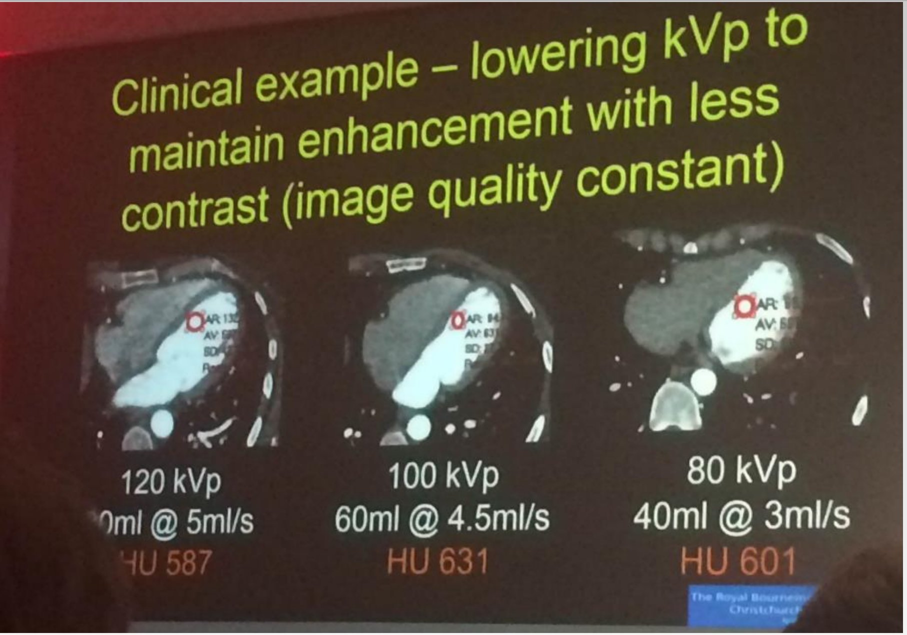

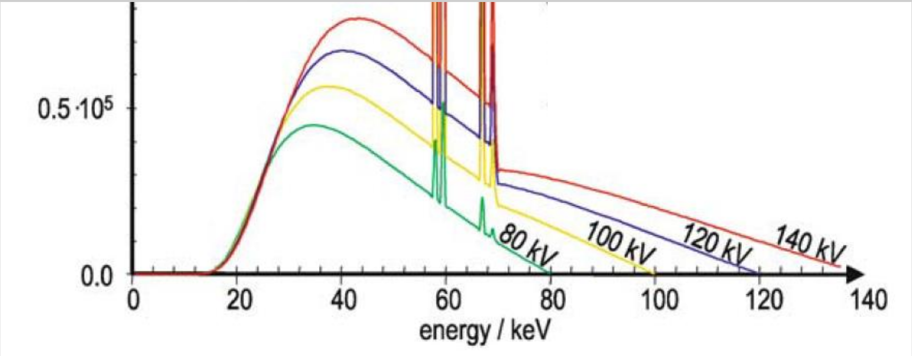

At 80 kVp there are many 30-35 keV photons which are absorbed very strongly by iodinated contrast (k-edge = 33.2 keV) *“qualità delle immagini”*

Note:

- Per lo stesso valore di SD, è possibile modificare il comportamento del «NPS»
- Visivamente l'uomo è sensibile alla composizione spettrale del rumore

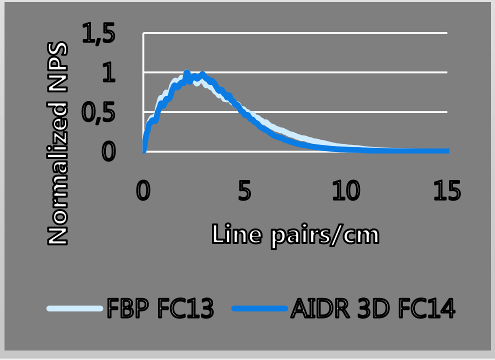

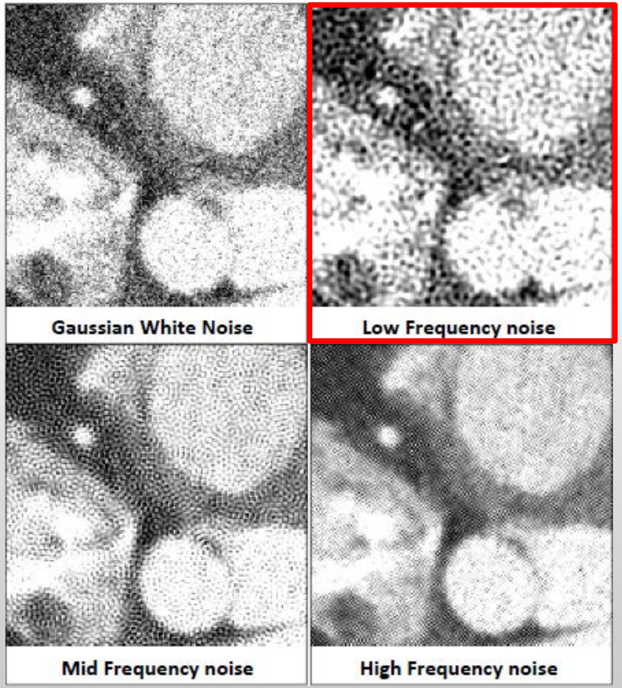

FIRST (MBIR)

Forward Projected Model-Based Iterative Reconstruction SoluTion

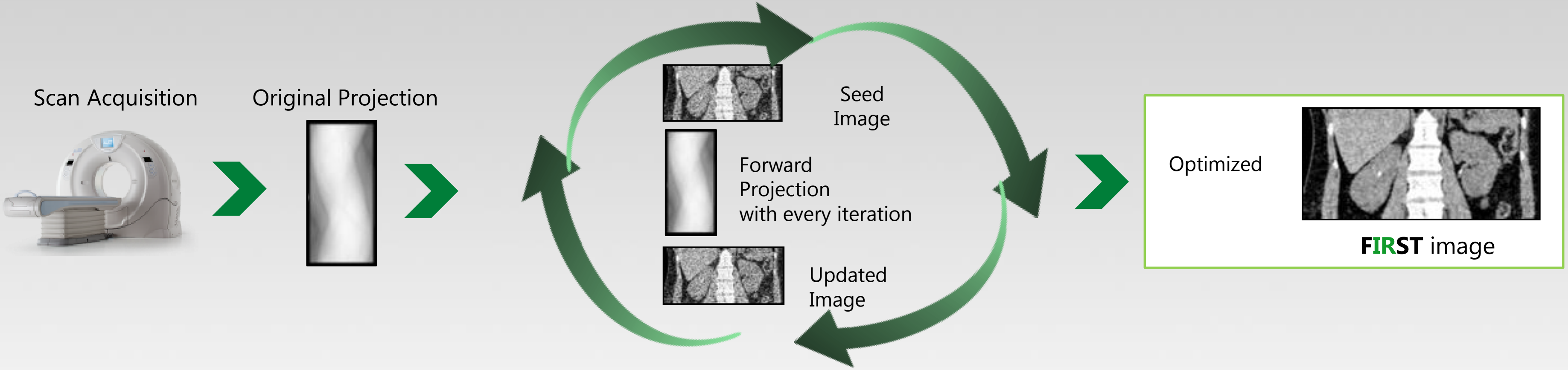

Model Based Iterative Reconstruction:

- Integrated and easy to use
- Automated
- Fast

FIRST (***F***orward projected model-based ***I***terative ***R***econstruction ***S***olu***T***ion)

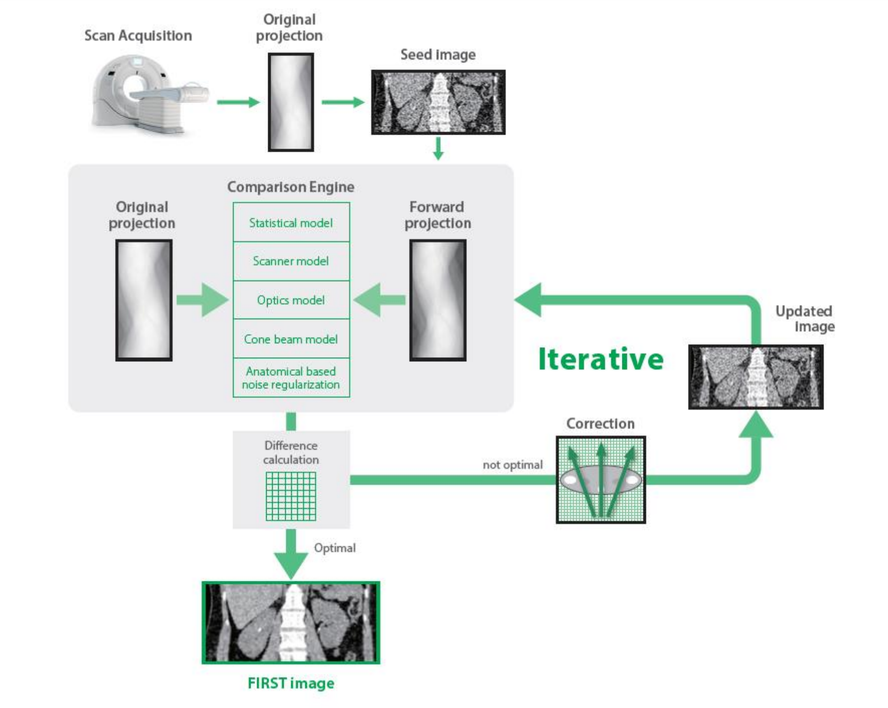

FIRST **(*F*orward projected model-based *I*terative *R*econstruction *S*olu*T*ion)**

1. No more kernel but different algorithms
   - » *Body* and *Cardiac* for soft tissues
   - » *Bone* for high contrast structures
   - » *Lung*
   - » *Brain*

2. Works for both Volume and Helical acquisition
3. Integrated into SUREExposure ensuring automatic dose reduction
4. Parallel reconstruction (AIDR 3D & FIRST) with fast reconstruction time (±3 min/vol)

Image quality improvement

FIRST results in:

- » Improved SNR at low dose
- » Improved Spatial Resolution

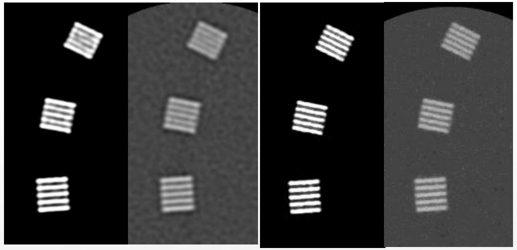

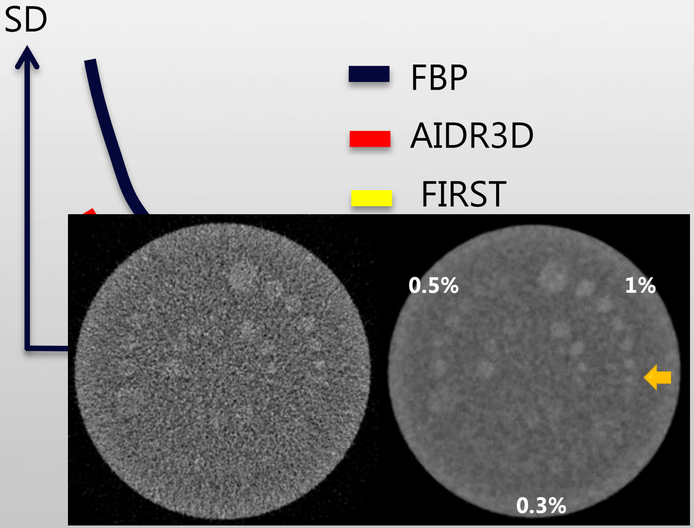

Low Contrast Phantom FBP vs FIRST (50mAs)

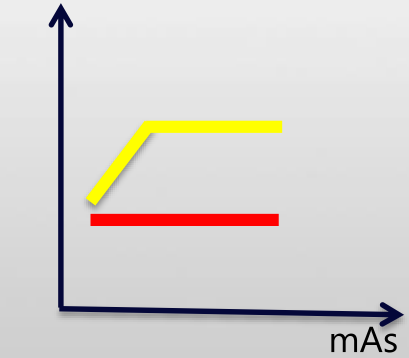

83 y.o. man, 80kg, BMI=28.7. Anticoagulant-related subcapsular liver hemator

FBP | AIDR 3D | **FIRST**

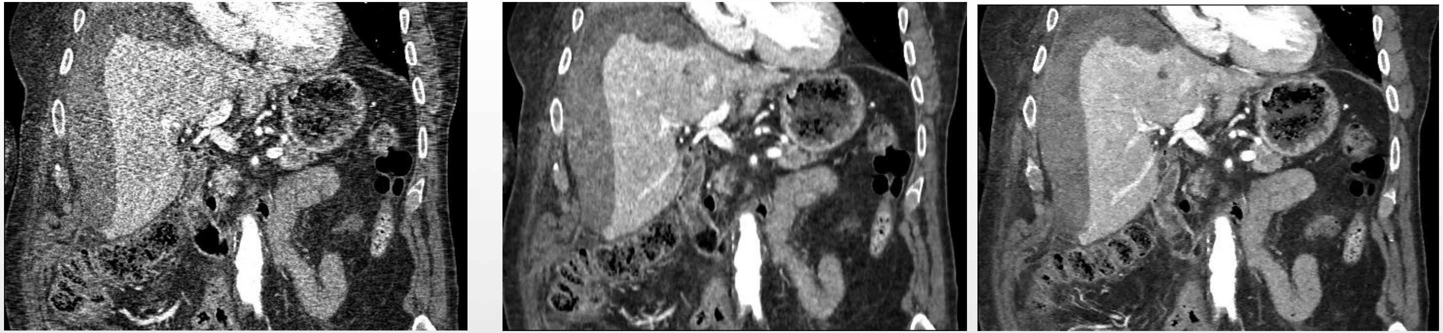

DLP = 214 mGy.cm, 3.2 mSv

DLP = 75 mGy.cm, 1.1 mSv

Courtesy of Prof. Blum, Nancy University Hospital, France.

Carotid artery stenting

FBP

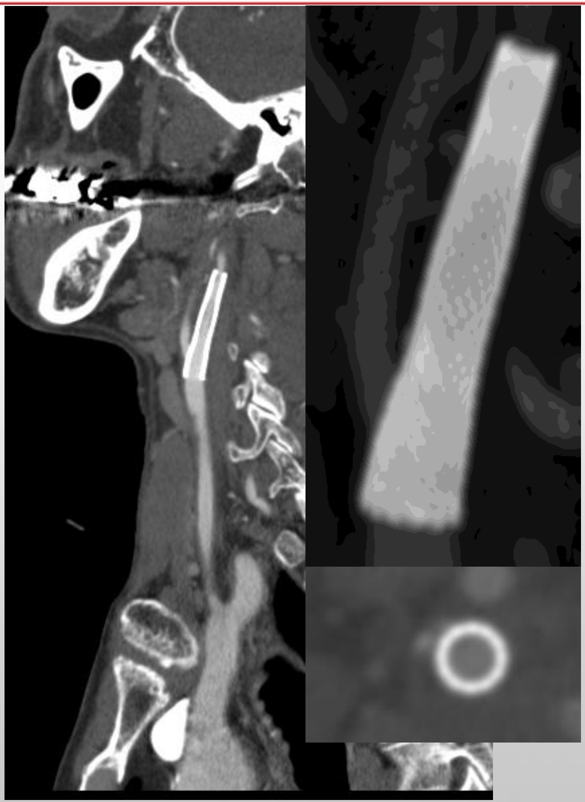

FIRST

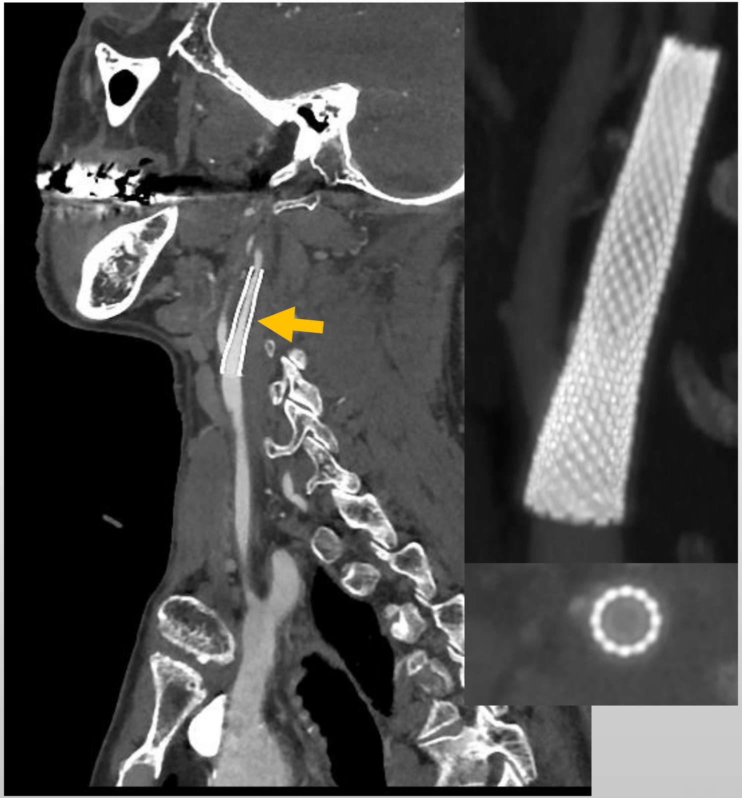

120kV / AEC50-250mAs /527.1 mGy.cm/3.1mSv

Courtesy of Prof. Awai. Hiroshima university hospital, Japan.

TOSHIBA MEDICAL

Follow-up after fixation of a OCD fragment in a 16 y.o. man

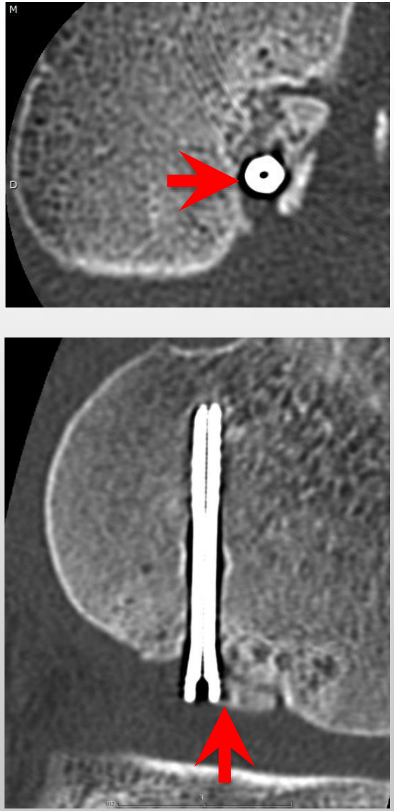

FC30 – AIDR 3D

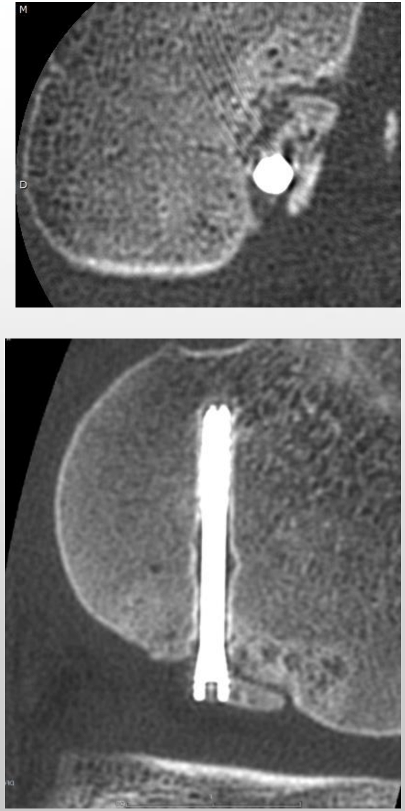

FIRST Bone

Courtesy of Prof. Blum, Nancy University Hospital, France.

Ultra-low-dose CT of the thorax

Literature suggests that

- 0.16 mSv are sufficient to detect > 3 mm nodules
- > 0.30 mSv are necessary to detect emphysema, ground-glass opacity nodules, nodules less than 3 mm

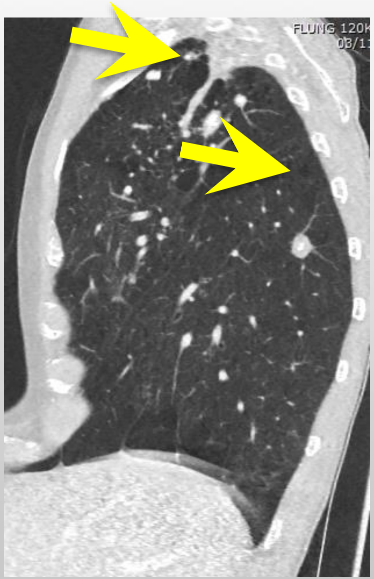

120kV, 3mAs, **FIRST** DLP = 13.5 mGy.cm, 0.19 mSv

TOSHIBA MEDICAL

Courtesy of Prof. Blum, Nancy University Hospital, France.

Sub-micro Sv CT for MSK

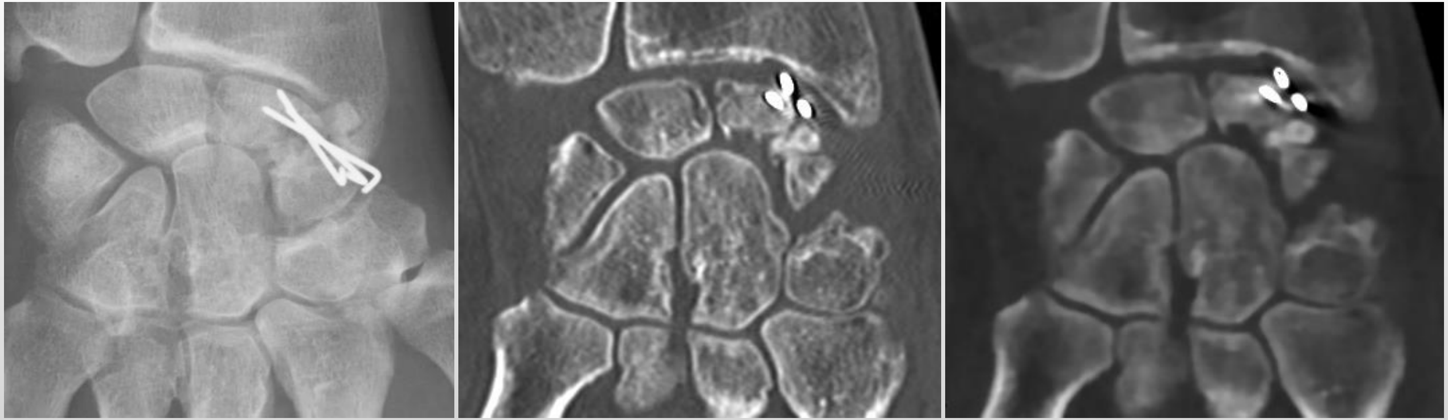

DLP = 15.9 mGy.cm, 3.5 μSv

DLP = 0.6 mGy.cm, 0.13 μSv

Courtesy of Prof. Blum, Nancy University Hospital, France.

imaging nella routine “sottrazione”

A bit of Subtraction history

- *'CT angiography with digital subtraction of extra- and intracranial vessels' - Gorzer et al; 1994*
  - 1st subtraction technique
  - N=26
  - Bone removal 100% success rate

  - Conclusion: Subtraction allows robust and fast selective elimination of bony structures and a better analysis of arteries at the level of the skull base. This is useful of both detection and therapy planning of intracranial aneurysms

Subtraction advantages

- CTA = ‘golden standard’ for vascular occlusive disease
- Problems:
  - Extensive calcium, stents
  - blooming artefacts
  - Overestimation of stenosis
  - False positive diagnosis of occlusion


Subtraction advantages

Original image

Subtracted image

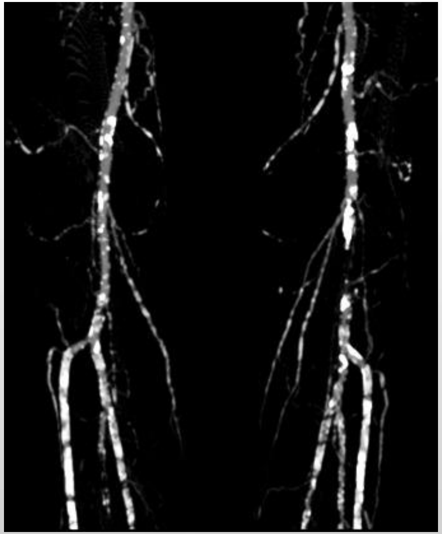

Original image

Subtracted image

Subtraction advantages

- Standard bone removal

Subtraction advantages

- ➢ Standard bone removal

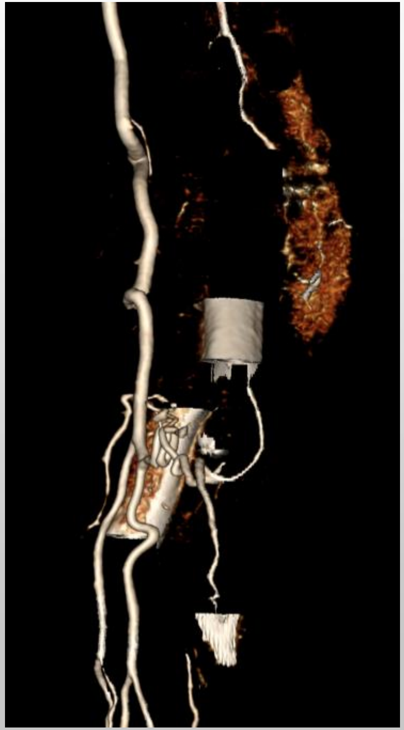

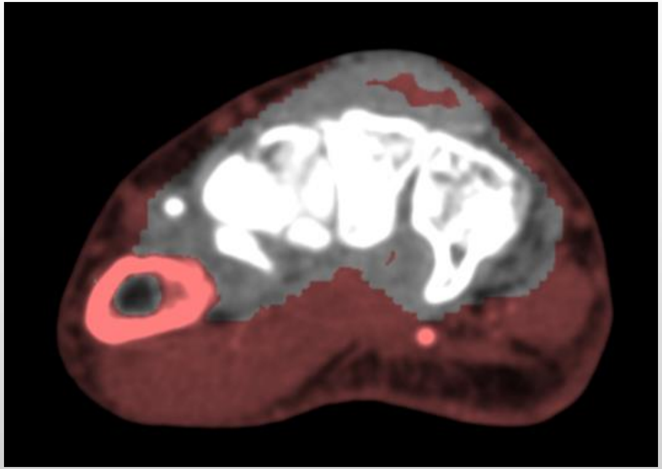

Body Perfusion

Deformable Registration

Registrazione deformabile calcola le differenze tra ogni singola immagine clinica e compensa il cambiamento di forma e di spostamento della posizione dovuti al movimento anatomico durante il processo di scansione.

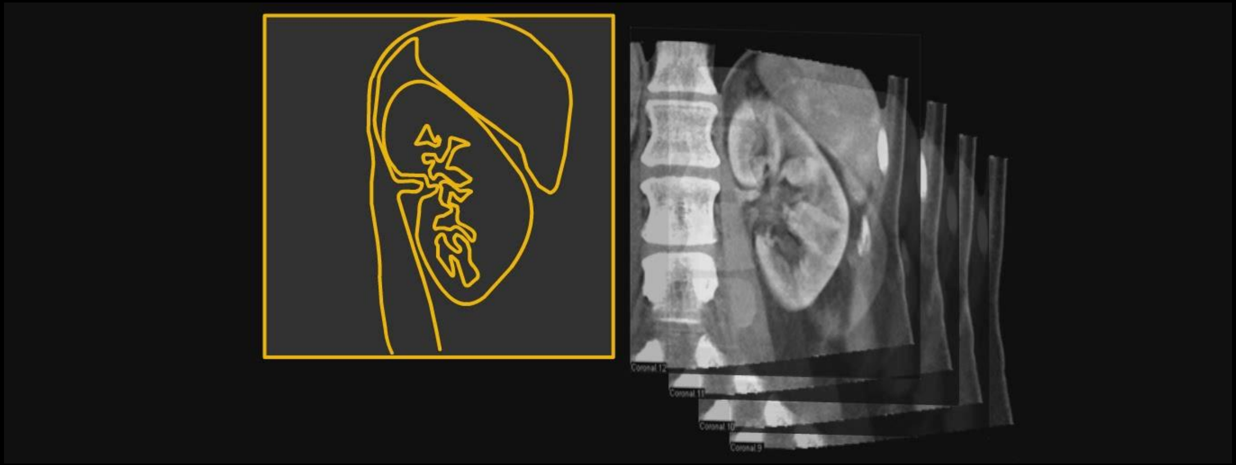

Subtraction CTA

- Rigid or non-rigid registration?
  - 26-y-o female with calcified chondroma para-vertebral

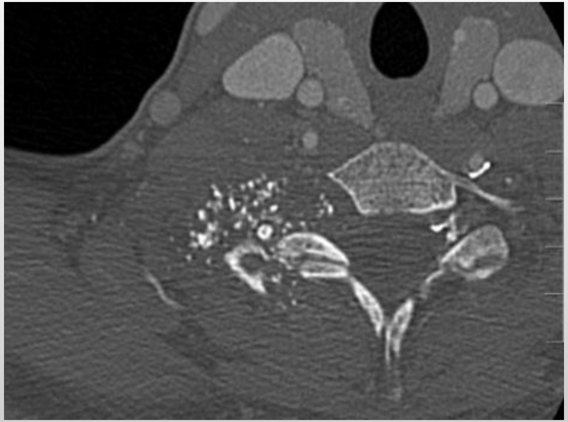

CT-Perfusion

Rigid Registration

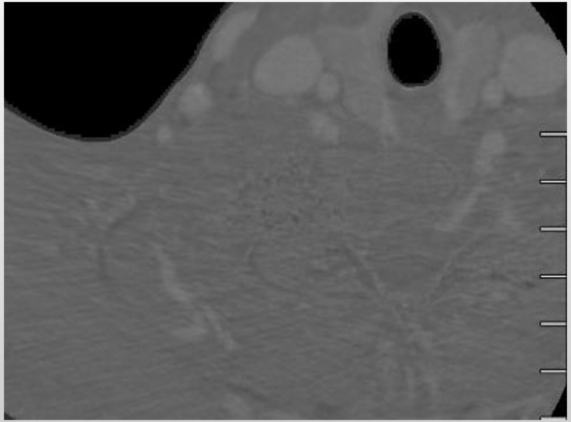

Non-Rigid Registration

Subtraction advantages

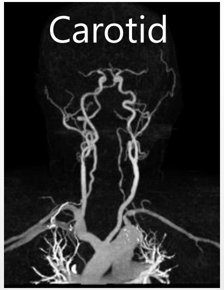

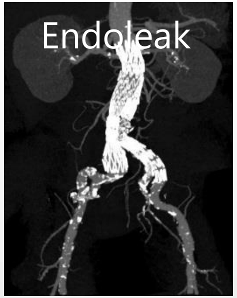

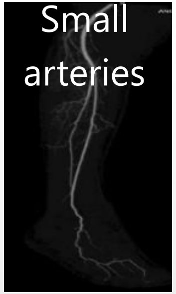

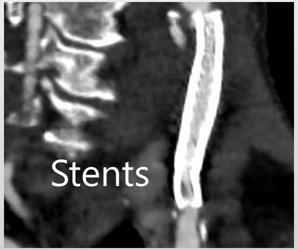

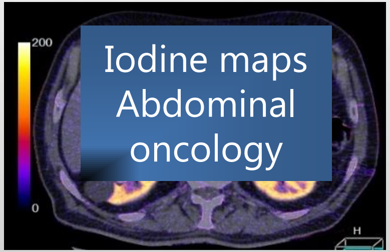

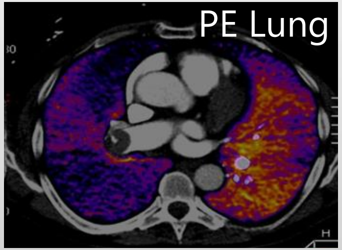

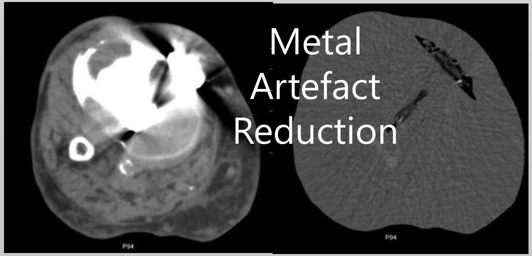

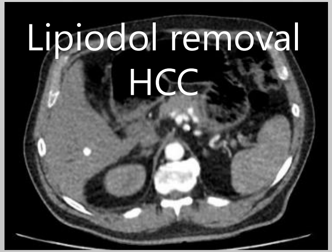

Subtraction advantages

- DSA-like Subtraction
  - Removal calcifications & blooming
  - Removal streak artefacts from stents, clips
  - Better visualization of lumen
  - Increased reader confidence
  - Zero click post-processing

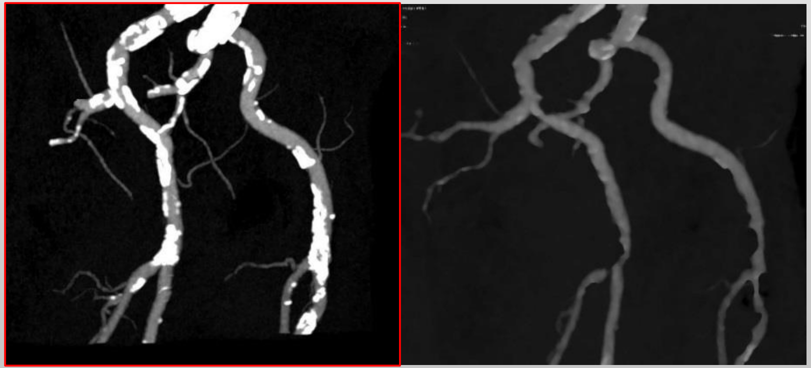

Subtraction CTA

Courtesy University Hospital of Strasbourg, Pr. Roy

- Case 2: 60-y-o patient 3 stents

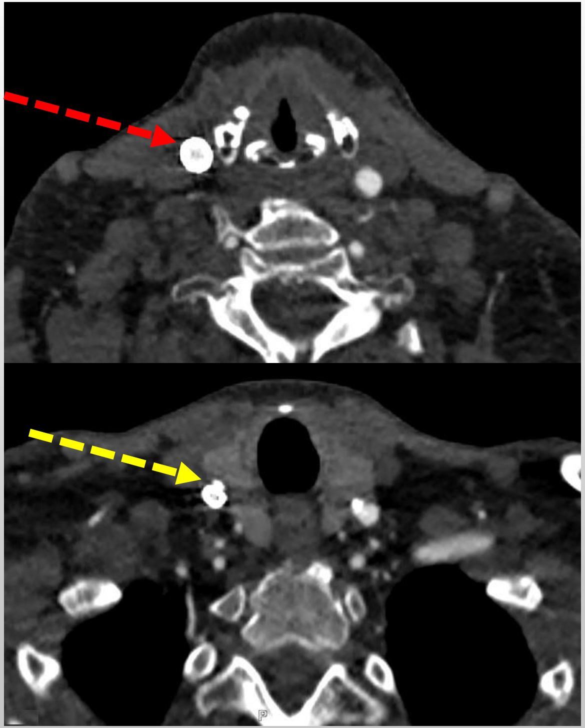

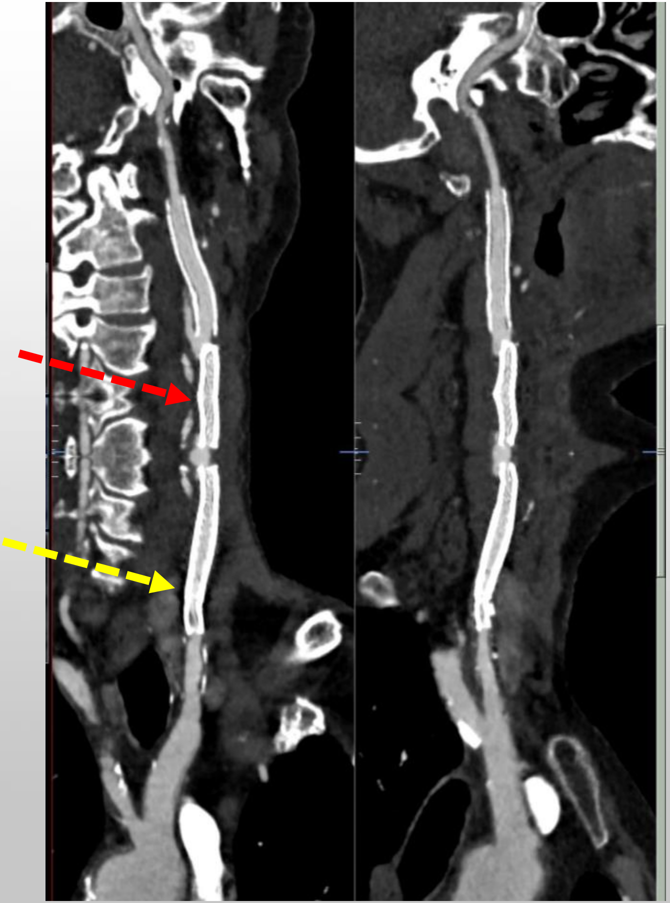

Subtraction CTA

Courtesy University Hospital of Strasbourg, Pr. Roy

- Does subtraction help us in this very difficult case?

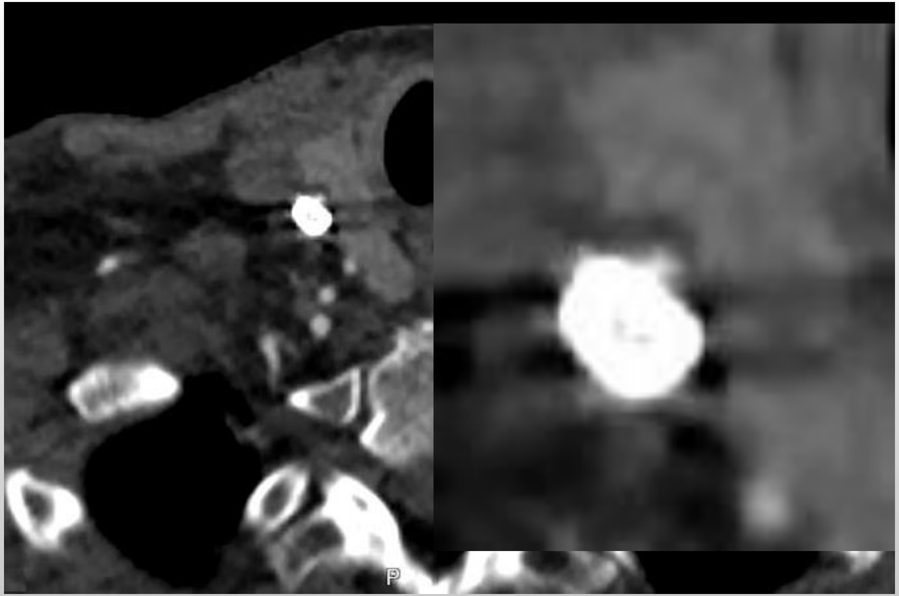

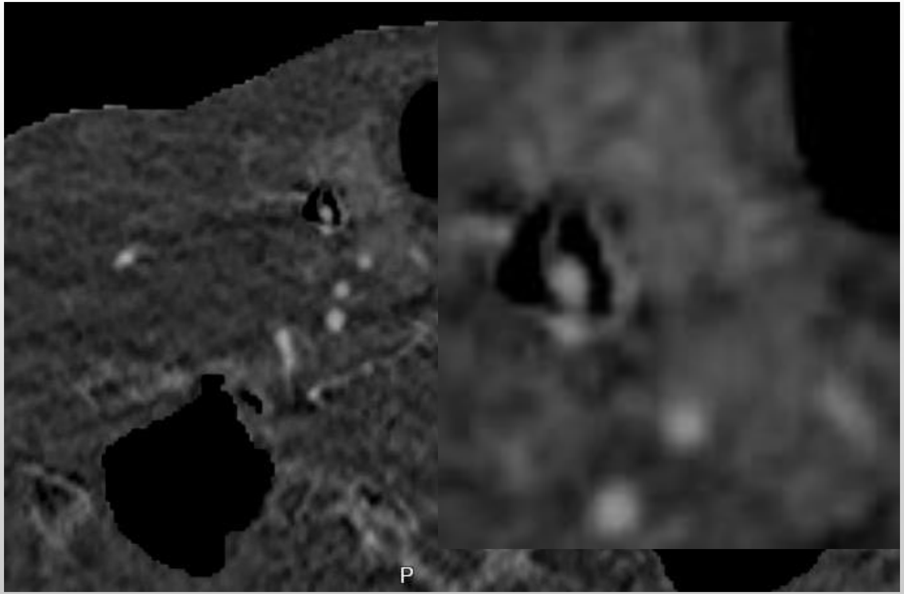

Subtraction CTA

Courtesy University Hospital of Strasbourg, Pr. Roy

- Does subtraction help us in this very difficult case?

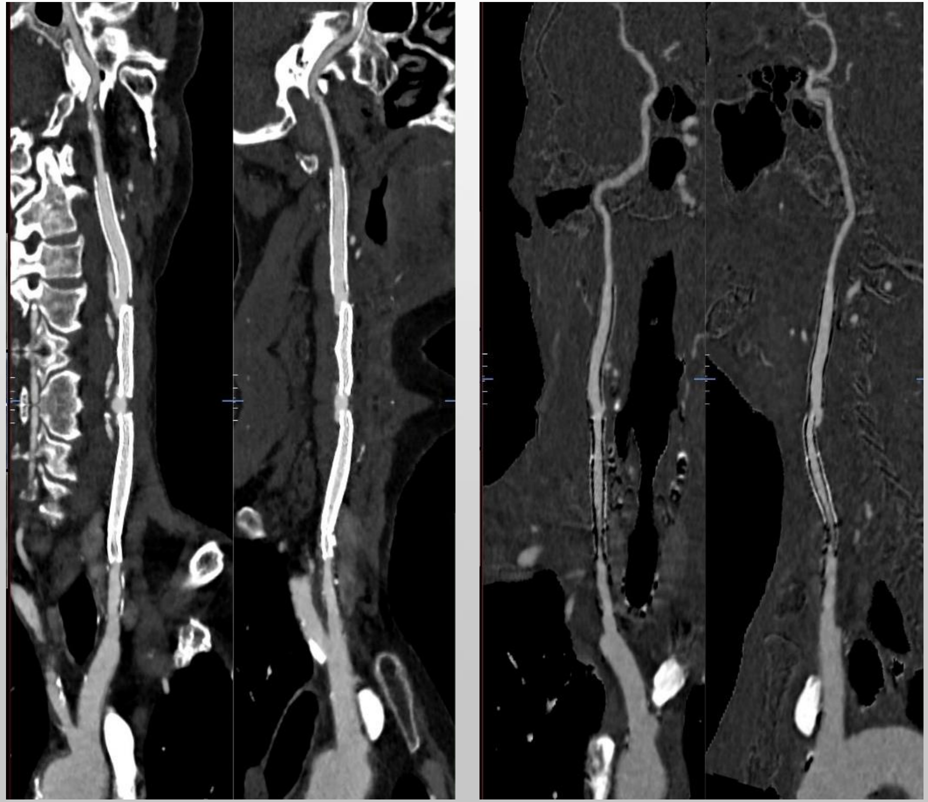

Subtraction CTA

Courtesy University Hospital of Strasbourg, Pr. Roy

- Increased reader confidence
- Confirms re-stenosis right ICA
- Stenosis measurement more accurate

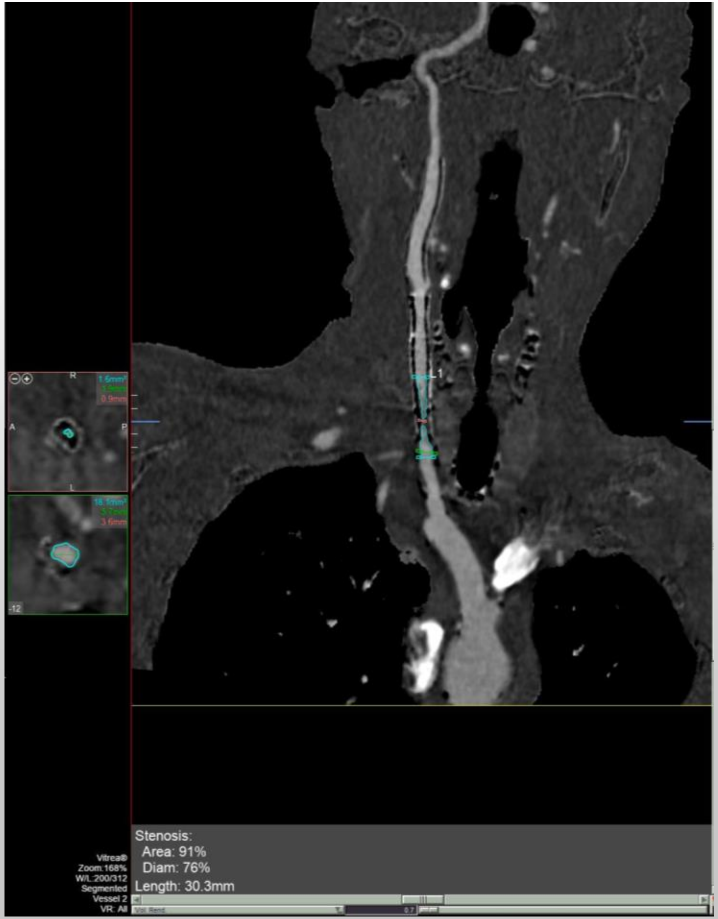

Subtraction CTA

Courtesy University Hospital of Nancy, Pr. Blum

- Case 3: 80-y-o. Surgery in 2019 for giant cell tumor.
  - Recurrance 2012. Radiotherapy. Follow-up

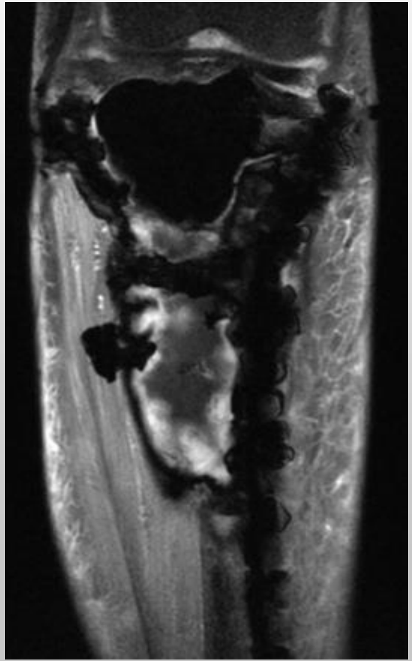

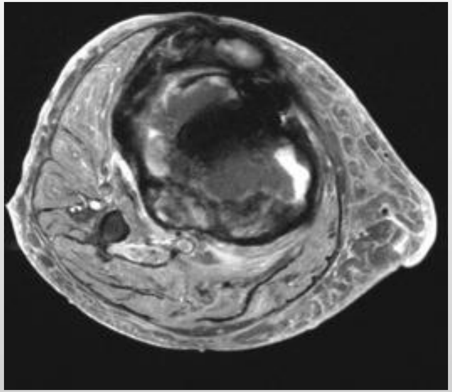

MRI IDEAL (Dixon) Fat suppression sequence

Subtraction CTA

Courtesy University Hospital of Nancy, Pr. Blum

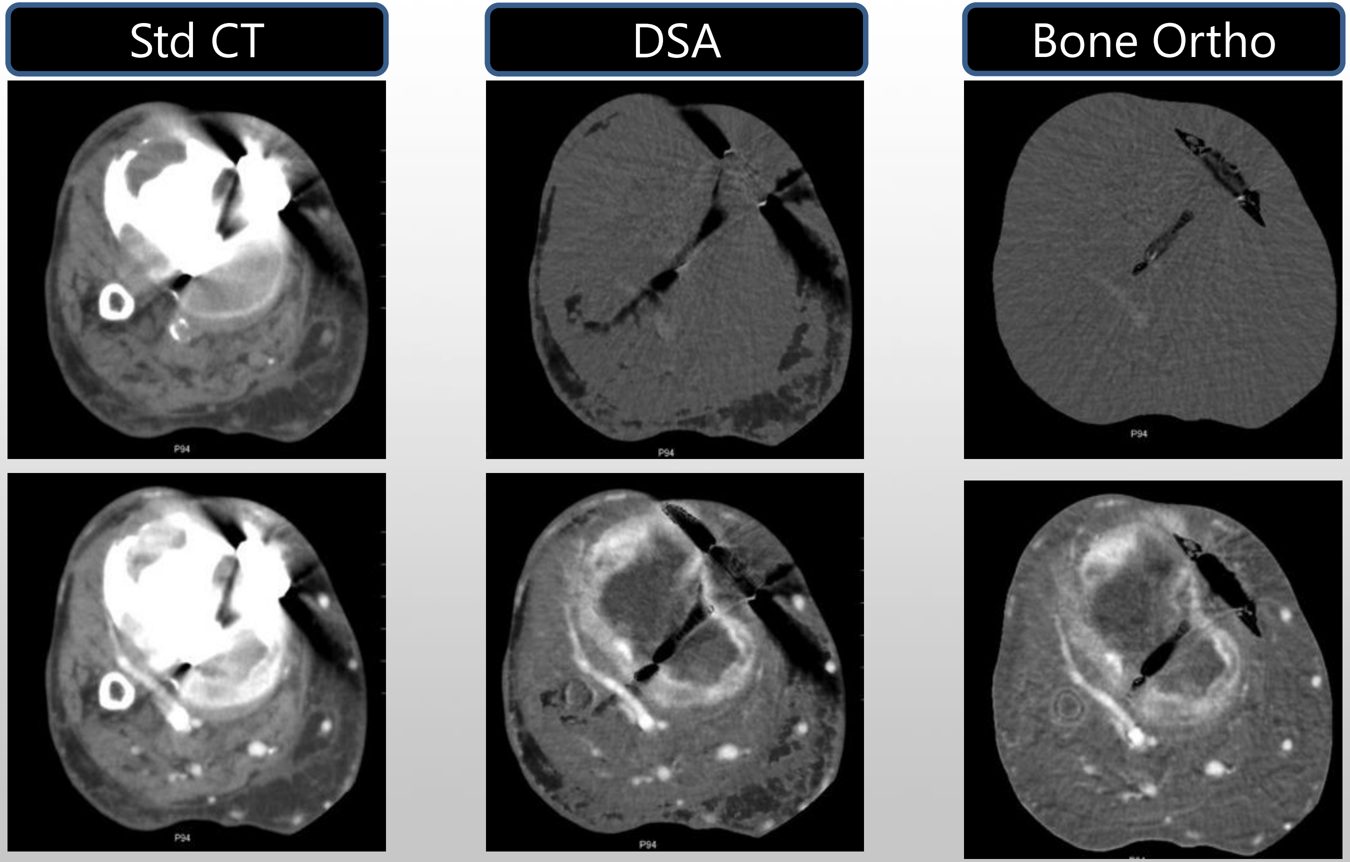

Subtraction CTA

Courtesy University Hospital of Strasbourg, Pr. Roy

- Case 4: 71-y-o female. Stent in left renal artery

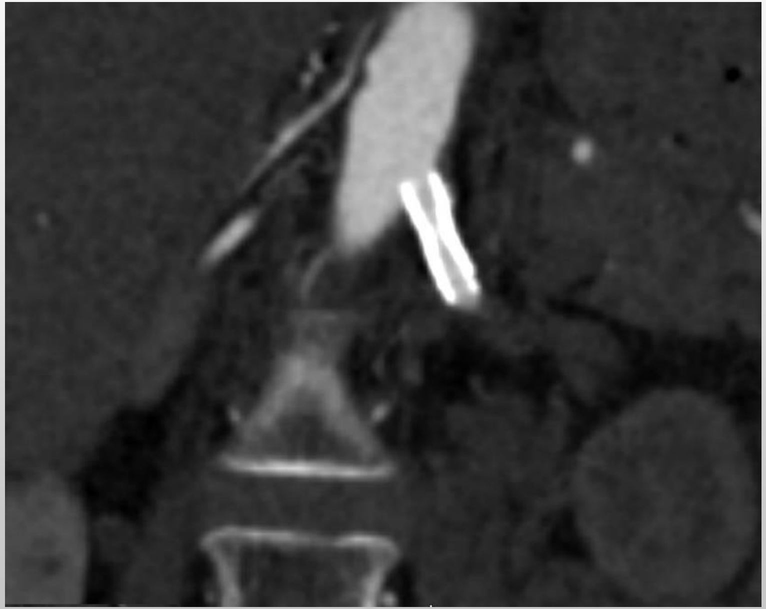

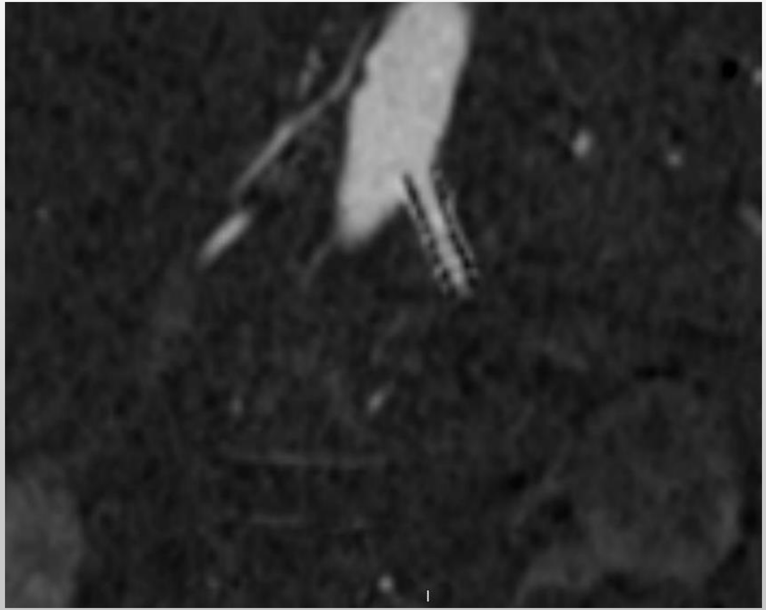

Subtraction CTA

Courtesy University Hospital of Strasbourg, Pr. Roy

- Case 8:
  - More small peripheral arteries
  - Improves contrast resolution
  - Confirmation no distal stenosis

LAD Calcification

Pre Contrast

Post Contrast

Courtesy Dr K Kofoed, Rigshospitalet, Denmark

LAD Calcification

- No hemodynamically significant stenosis is seen.

CTA

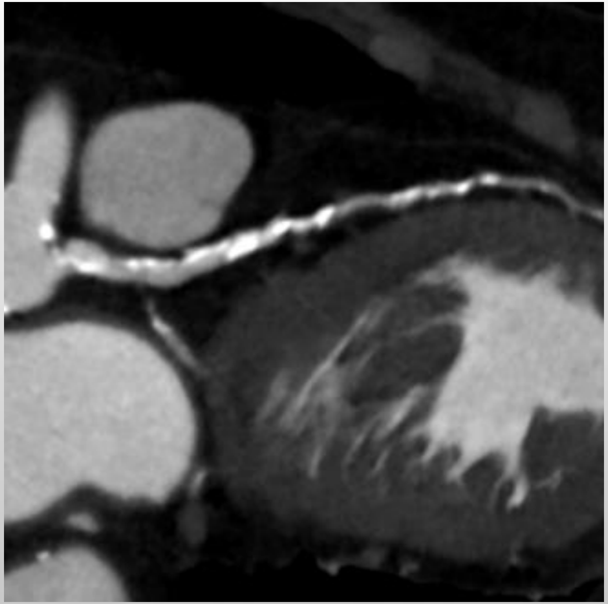

Subtracted

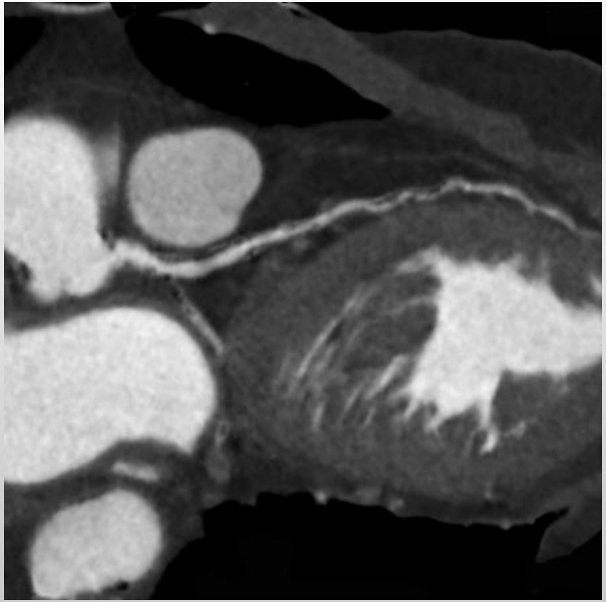

Courtesy Dr K Kofoed, Rigshospitalet, Denmark

LAD Calcification

- No hemodynamically significant stenosis is seen.

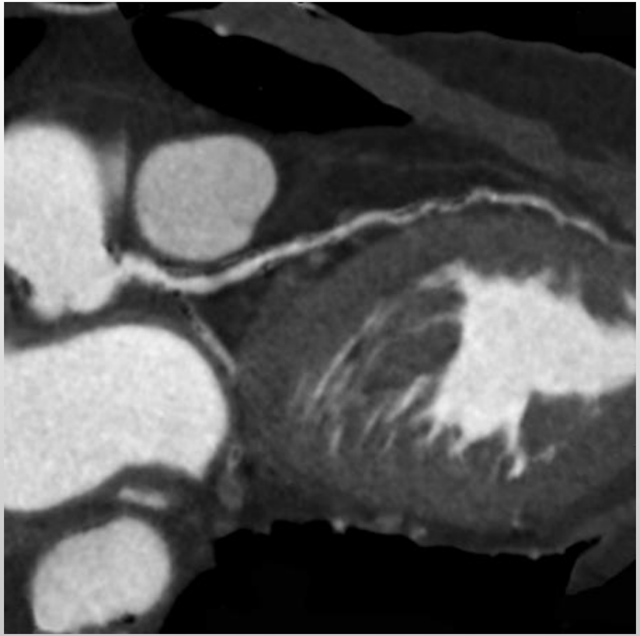

Courtesy Dr K Kofoed, Rigshospitalet, Denmark

In stent Re-stenosis

- In stent re-stenosis is seen in the LAD.

Post Contrast

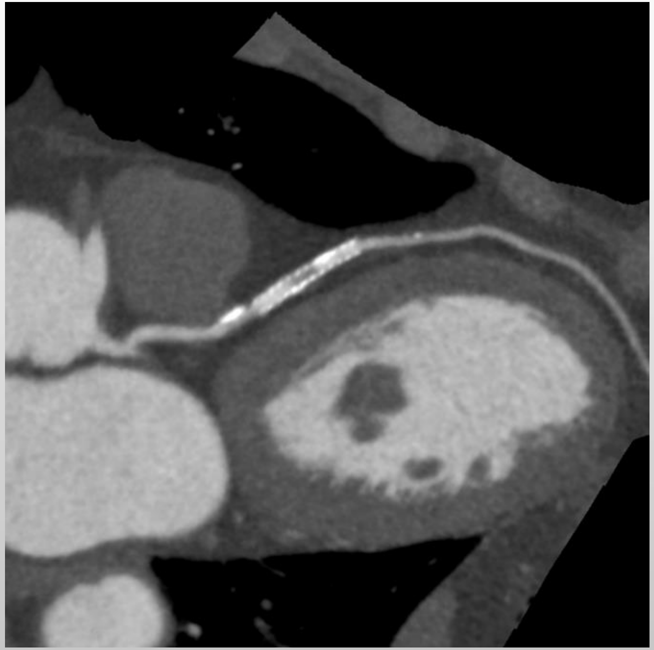

Subtracted

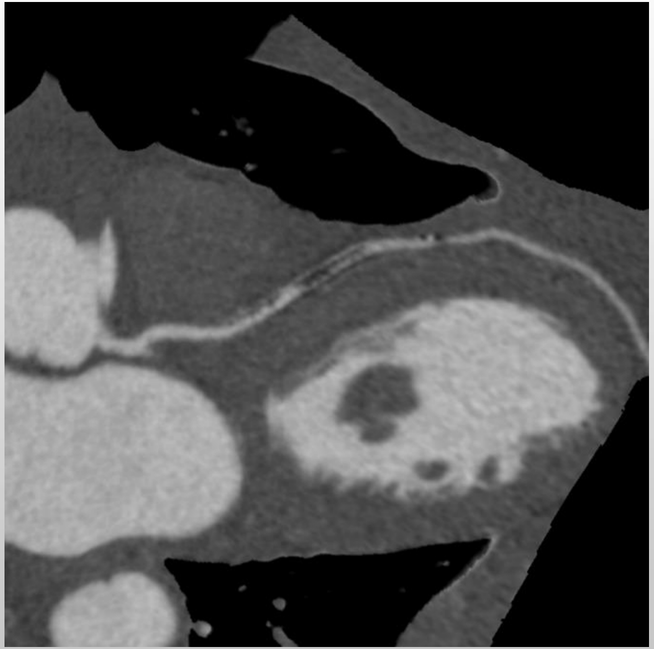

Courtesy Dr M Chen, NHLBI, National Institutes of Health, USA

In stent Re-stenosis

- In stent re-stenosis is seen in the LAD.

Subtracted

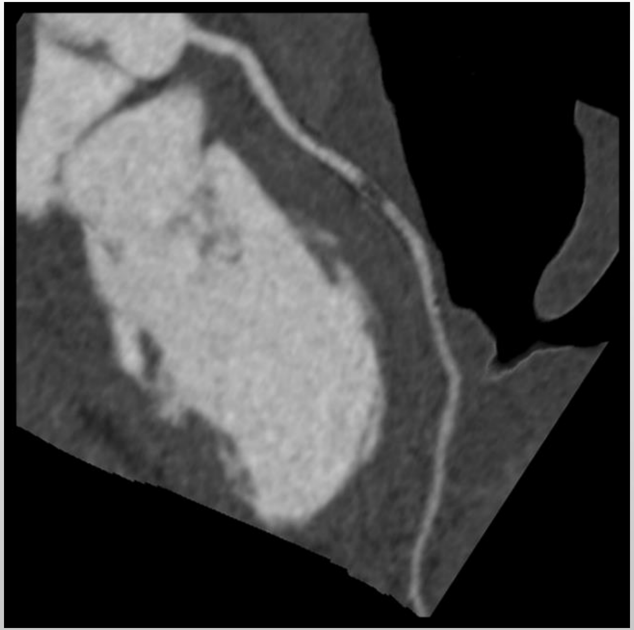

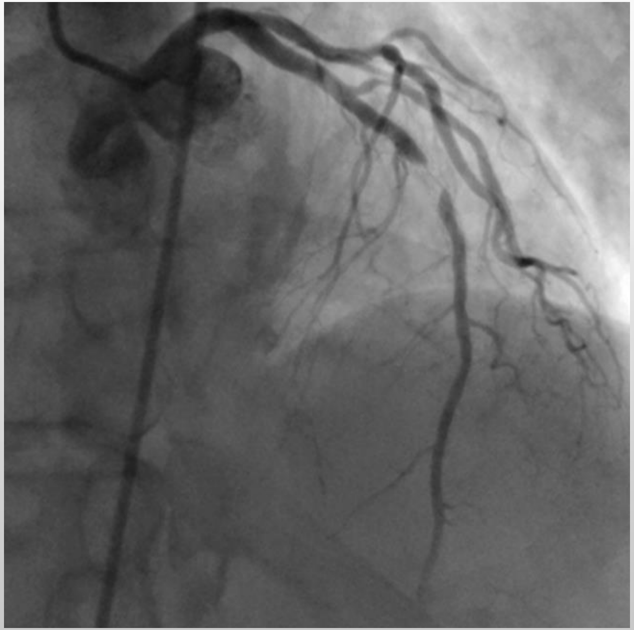

Courtesy Dr M Chen, NHLBI, National Institutes of Health, USA

Validation

- Subtraction Coronary CT Angiography for the Evaluation of Severely Calcified Lesions Using a 320-Detector Row Scanner, Yoshioka K & Tanaka R, *Current Cardiovascular Imaging Reports, 2011; 4(6):437-446*

- Subtraction Coronary CT Angiography for Calcified Lesions, Yoshioka K, Tanaka R, Muranaka K.Y, *Cardiol Clinics, 2012; 30(1):93-102*

- Improved evaluation of calcified segments on coronary CT angiography: a feasibility study of coronary calcium subtraction, Tanaka R, Yoshioka K, Muranaka K, Chiba T, Ueda T, Sasaki T, Fusazaki T, Ehara S, *International Journal of Cardiovascular Imaging*, 2013, Epub.

- Accurate Registration of Coronary Arteries for Volumetric CT Digital Subtraction Angiography, M. Razeto, J. Matthews, S. Masood, J. Steel, K. Arakita, *Proc. SPIE* Vol. 8768, 2013.

Subtraction CTA

- Case 10:
  - Iodine map differentation between tumor and cyst

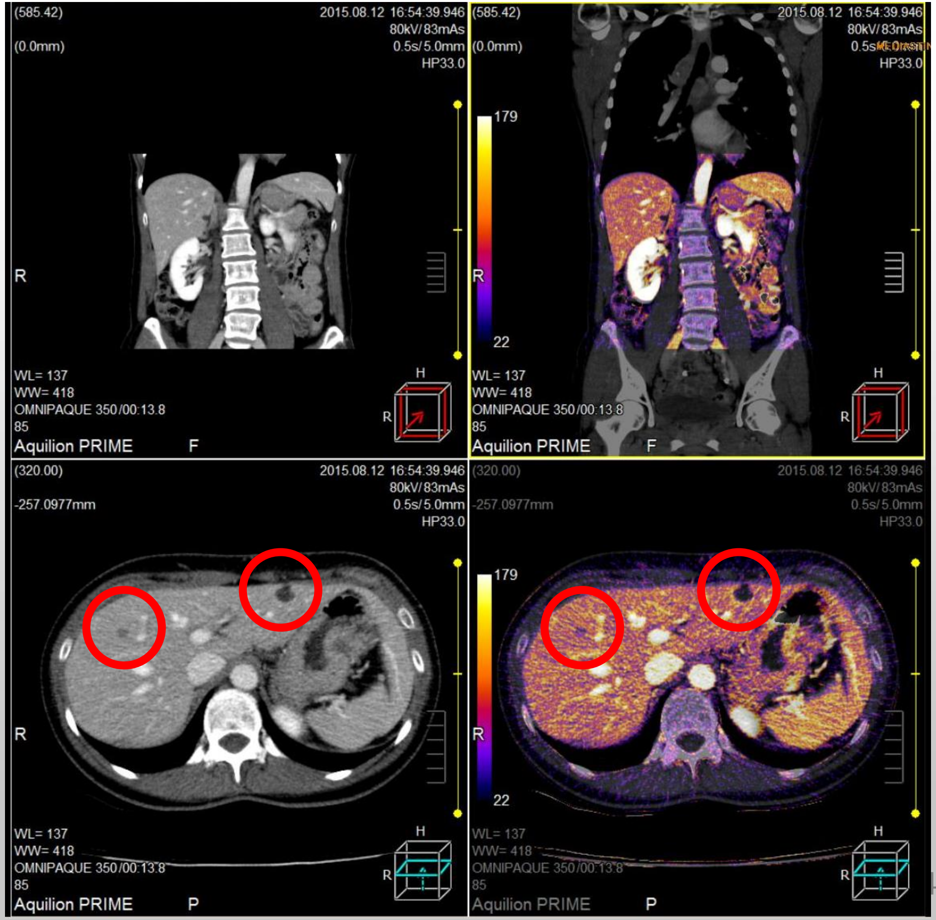

Dual Energy

Exploits different kV-dependence

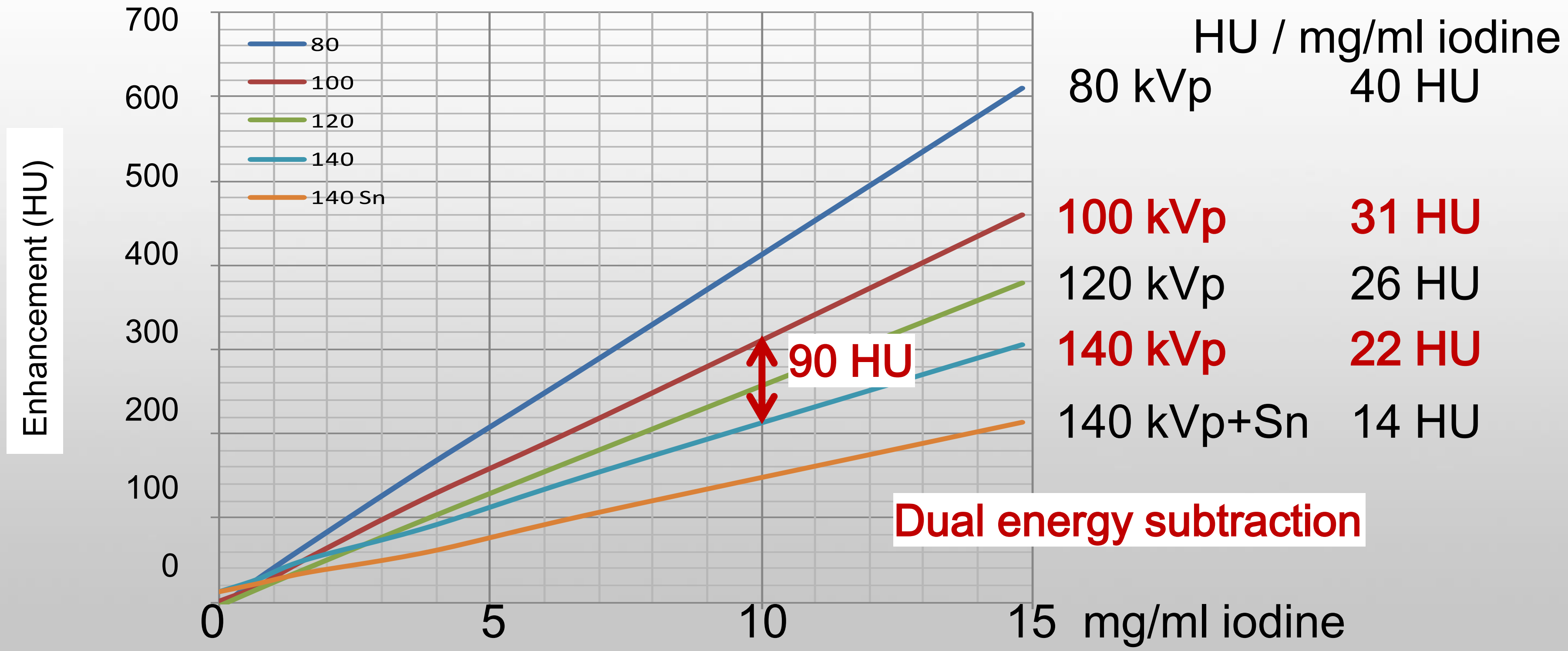

Subtraction Imaging

Exploits total iodine signal

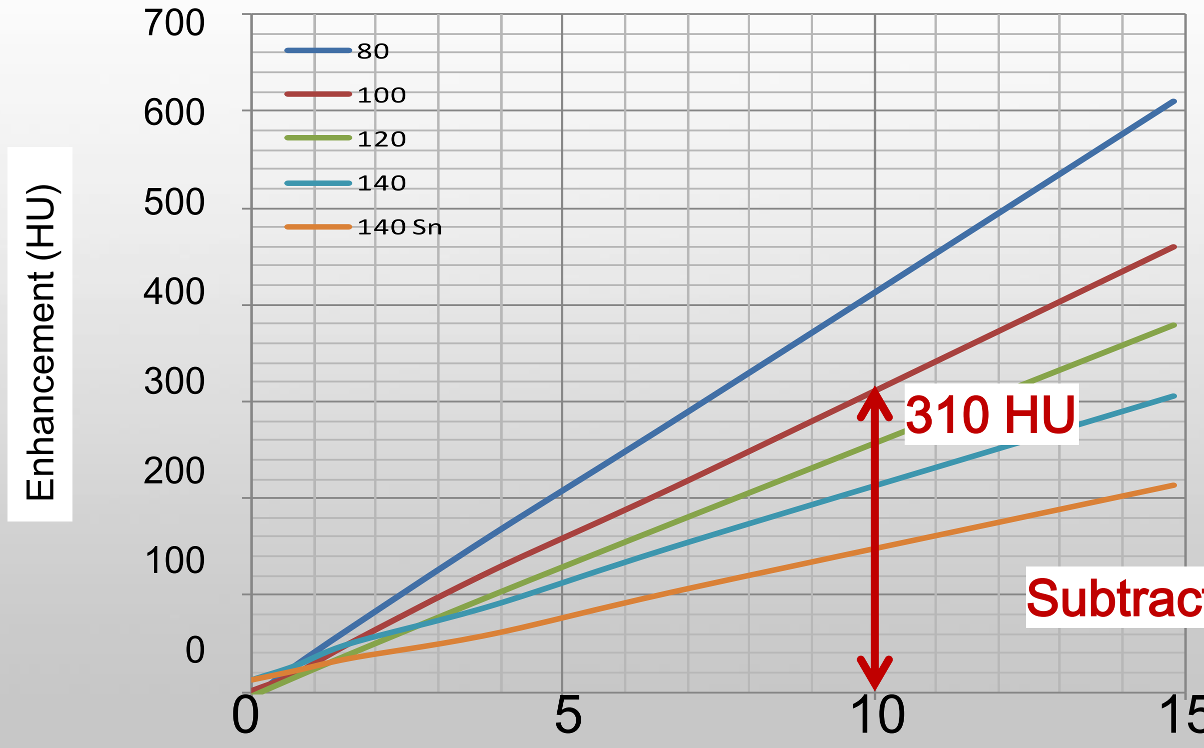

	HU / mg/ml iodine
80 kVp	40 HU
100 kVp	**31 HU**
120 kVp	26 HU
140 kVp	22 HU
140 kVp+Sn	14 HU

Subtraction imaging
3.4 x higher signal !

Clinical evidence (scientific)

LL-CHE4249

Education Exhibits

Iodine Mapping of the Lung Using Subtraction Imaging for Pulmonary Embolism: Technique and Initial Clinical Experience

PARTICIPANTS:

Monique Brink MD, PhD: Speaker, Toshiba Corporation
Eva M Van Rikxoort PhD **(Presenter)**: Nothing to Disclose
Jean Paul Charbonnier: Nothing to Disclose
Sarah J Van Riel MD: Nothing to Disclose
Cornelia M Schaefer-Prokop MD: Advisory Board, Riverain Technologies, LLC
Mathias Prokop MD, PhD: Speakers Bureau, Bayer AG Speakers Bureau, Bracco Group Speakers Bureau, Toshiba Corporation Speakers Bureau, Koninklijke Philips Electronics NV Research Grant, Toshiba Corporation

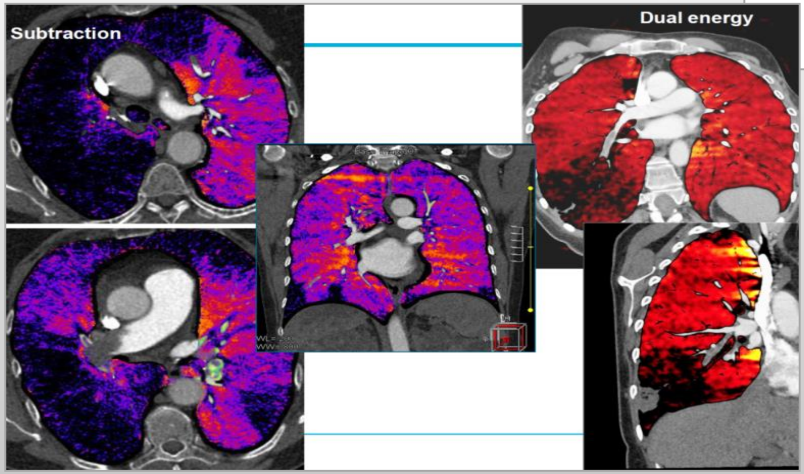

Clinical benefits:

"This subtraction technique allows for excellent evaluation of lung parenchyma and pulmonary vessels and achieves a more than 3 times higher contrast-to-noise ratio than dual energy images at identical dose."

Subtraction CTA or DE

Compare to Dual Energy, what's the best ?

- Comparison study: "Standard Bone Removal" Vs "Dual Energy Bone Removal"

Medical Physics
The International Journal of Medical Physics Research and Practice

Automated bone removal in CT angiography: Comparison of methods based on single energy and dual energy scans

Marcel van Straten[1,a)], Michiel Schaap[2], Marcel L. Dijkshoorn[3], Marcel J. Greuter[4], Aad van der Lugt[5], Gabriel P. Krestin[5] and Wiro J. Niessen[6]

Conclusions: Both techniques provided bone suppression in a fully automated way. DE provided more complete bone suppression in the neck, but at the cost of inferior vessel integrity, especially at the thoracic inlet. BSCTA showed excellent results for vessel integrity and was superior to DE in most of the vessels in or at the skull base.

Subtraction CTA or DE

- Comparison study at CHU Strasbourg: Average dose for CTA Carotid
- [redacted] (Dual Energy) Vs **ONE VISION** (Subtraction)

Dual Energy (80 patients)	**Subtraction** (68 patients)
716mGy.cm	**270mGy.cm**

imaging nella routine “Dual Energy”

Dual Energy

- Dual Energy subtracts high energy data from low energy data

$$\hat{I} = N \int_0^{E_{max}} \mathrm{d}E\, \Omega(E)\, \eta(E) \exp\left[-A_1 \psi_1(E) - A_2 \psi_2(E)\right],$$

- So, DE is a kind of subtraction........

Dual Energy

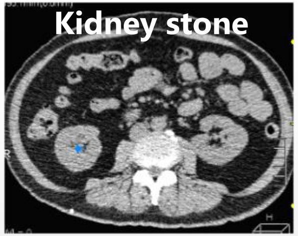
Kidney stone

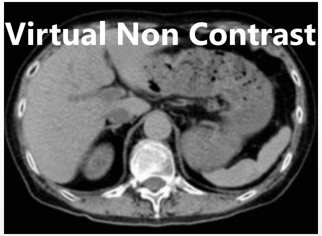
Virtual Non Contrast

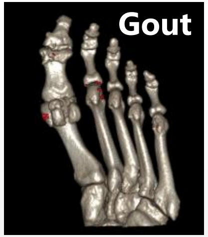
Gout

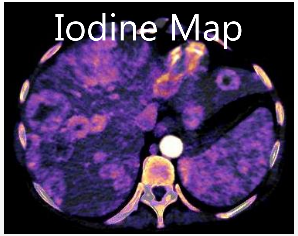
Iodine Map

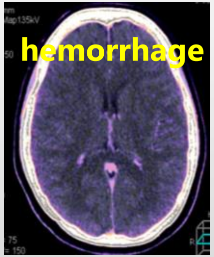
hemorrhage

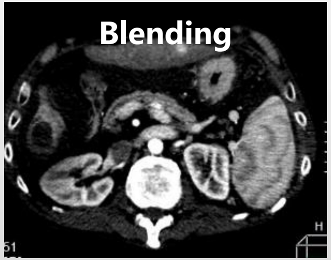
Blending

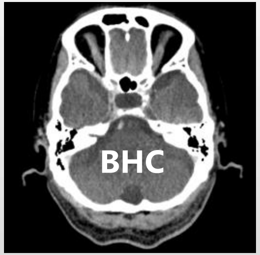
BHC

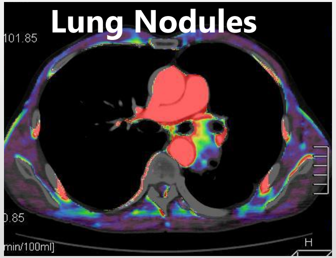
Lung Nodules

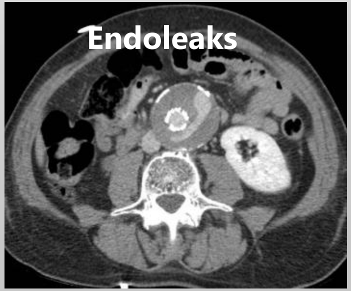
Endoleaks

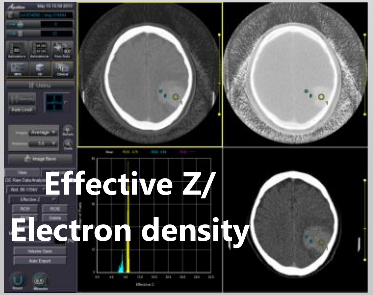
Effective Z/
Electron density

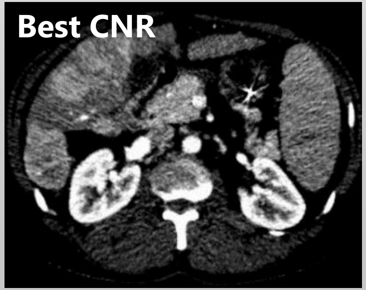
Best CNR


MSK

Dual Energy

- Case 11: DE follow-up treatment Nexavar* for HCC

Single energy 6 months post treatment

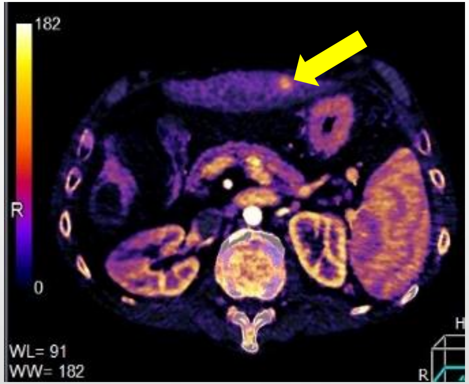

Iodine map

Blending

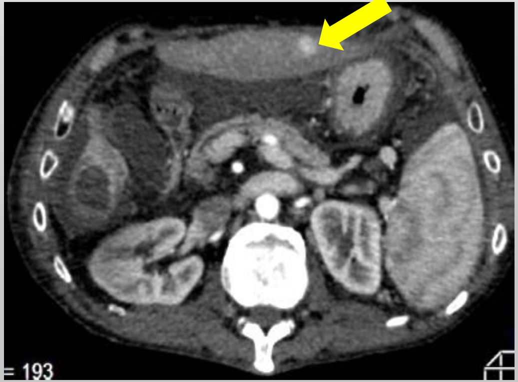

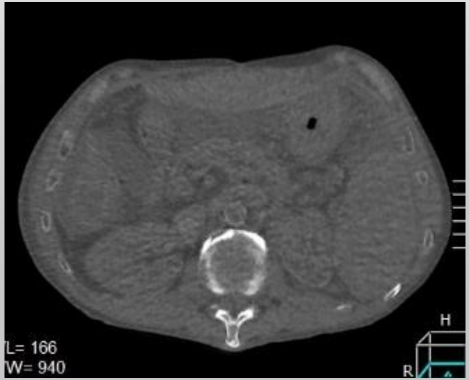

VNC

* Decreases tumor growth; anti-angiogenesis

Dual Energy

- Case 12: 71-y-o male. Pre-treatment evaluation mass in paranasal sinus

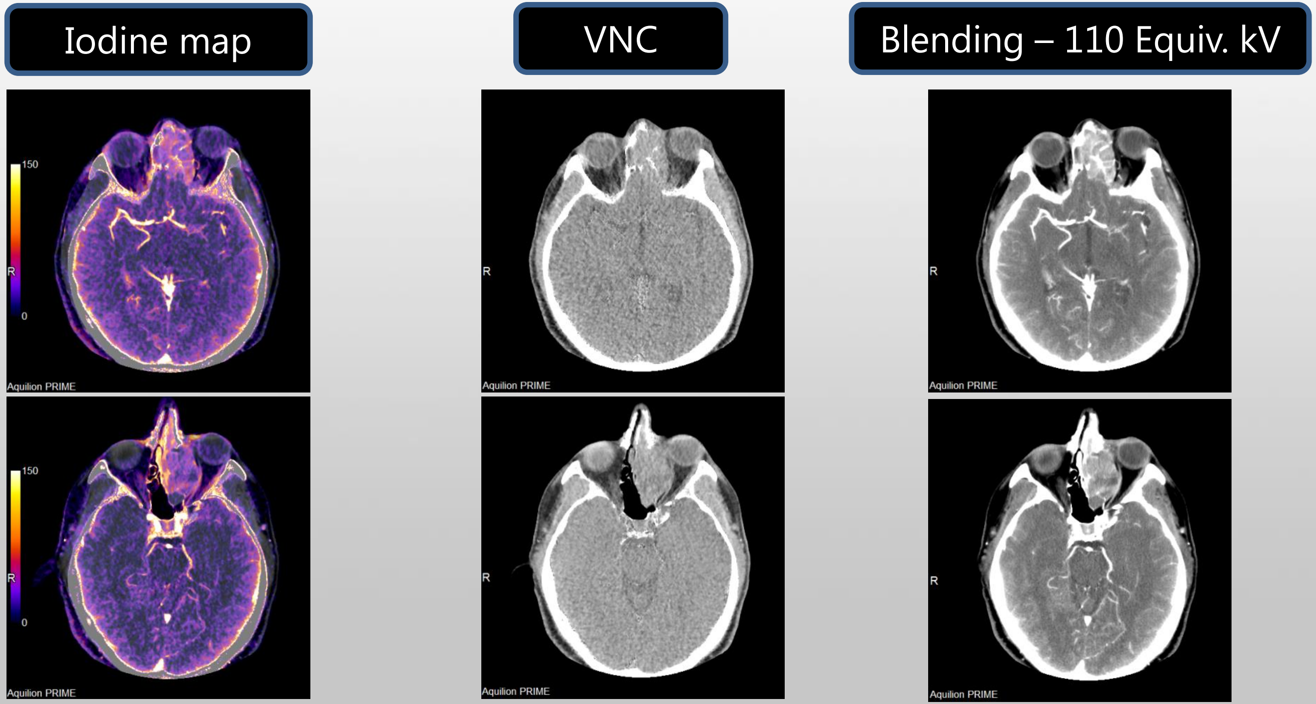

Endourology and Stones

Impact of Reduced-radiation Dual-energy Protocols Using 320-Detector Row Computed Tomography for Analyzing Urinary Calculus Components: Initial In Vitro Evaluation

Xiangran Cai, Qingchun Zhou, Juan Yu, Zhaohui Xian, Youzhen Feng, Wencai Yang, and Xukai Mo

MATERIALS AND METHODS

This prospective study enrolled 58 consecutive patients referred for assessment of urinary stone disease who were eligible for the study after they gave informed consent to our university hospital between January and November 2013.

A total of 58 stones were extracted from the 58 patients who underwent percutaneous nephrolithotripsy, open surgery, retroperitoneal laparoscopic pyelolithotomy, or ureterolithotomy. Patients' mean age was 39.7 ± 6.5 years (range, 16-72 years). Calculi were located in the renal pelvis and calices in 46 patients and in the ureter in 12 patients. Stone diameters varied between 5 and 28 mm (mean diameter, 13.6 mm). Analysis of

CONCLUSION

In this study, we were able to demonstrate the feasibility of compound analysis of urinary stones with low-dose DE-CT. Compared with chemical analysis, and with XRD serving as a reference standard, we were also able to precisely differentiate calcified, uric acid, and cystine stones with 96.6% accuracy while allowing for patient dose savings of up to 50% (1.81 mSv) using 135 kV, 50 mA and 80 kV, 290 mA scan protocols. When the

Virtual Non Contrast

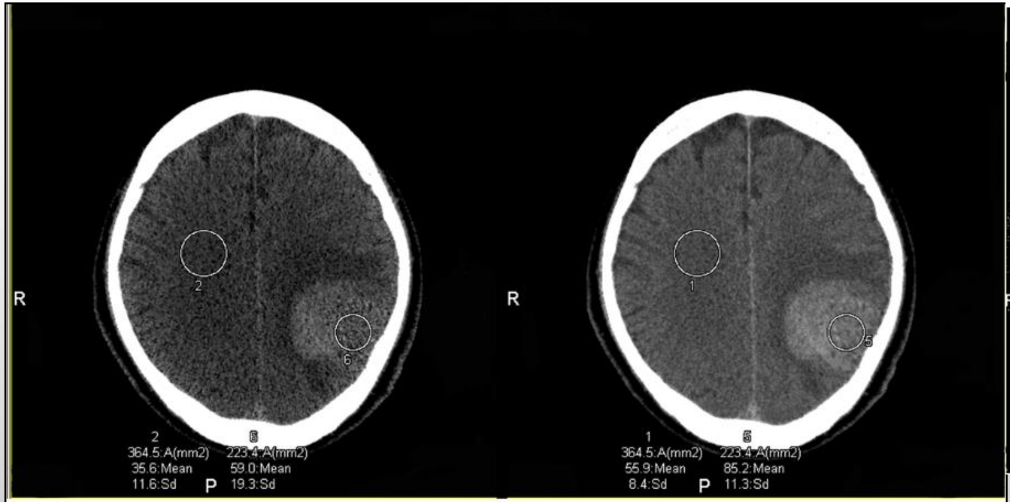

SD = 11.6
CNR = 2.0

SD = 8.4
CNR = 3.5

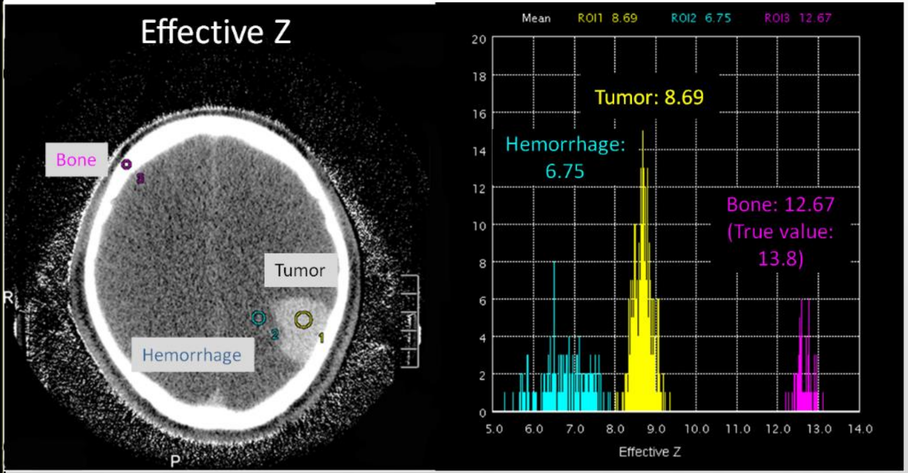

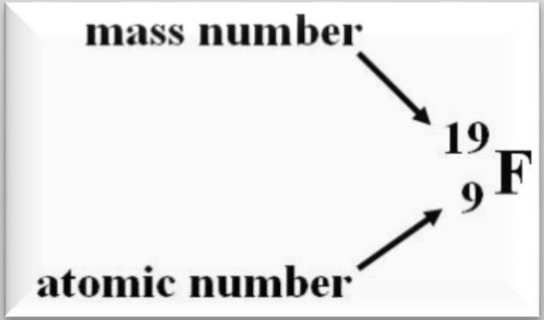

Source: "Dual Energy Raw Data Based Decomposition Analysis on Aquilion ONE", F. Tatsugami et al.

Toshiba's Raw data analysis

» One tube and one detector
» High energy (kVp) during one rotation followed by low energy during another rotation

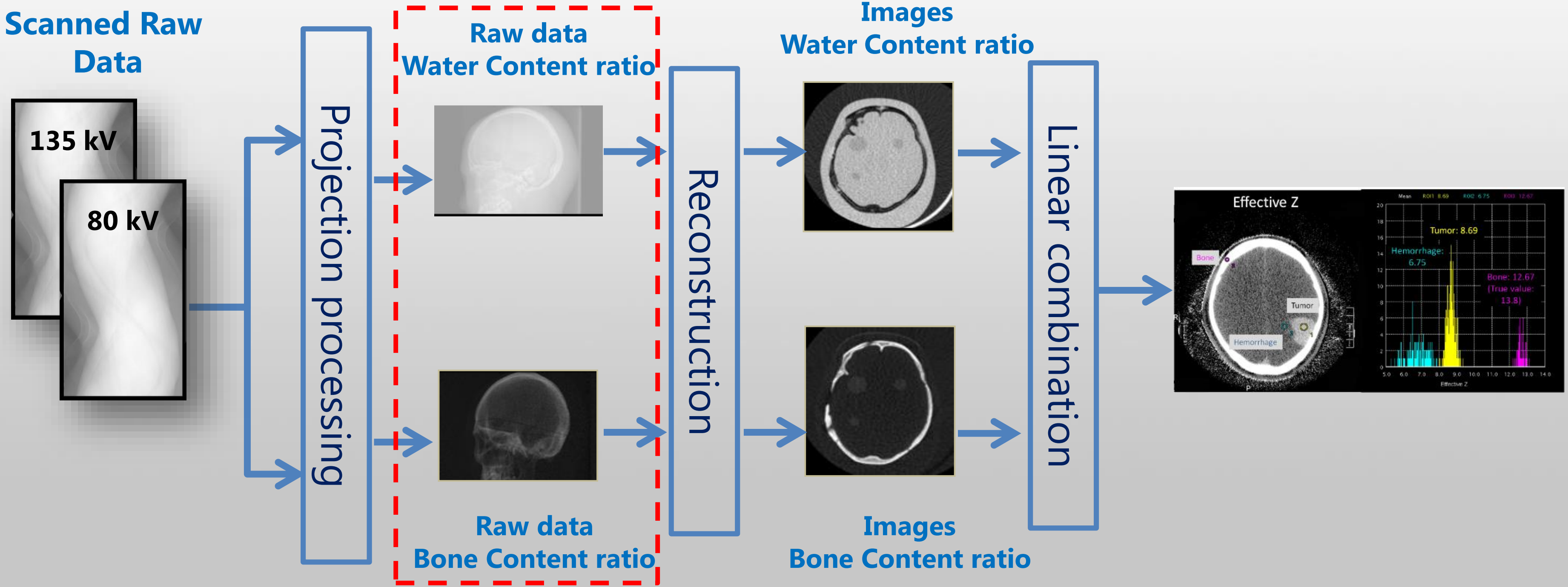

- One tube and one detector
- High energy (kVp) during one r

TABLE 2. True and Measured Effective Atomic Numbers and Errors Between True and Measured Values

Inset Number	Rod-Type Substitute		True Effective Atomic Number	Mean Measured Effective Atomic Number	Error, %
1	Adipose tissue	SZ-49	6.090	5.565	−8.62
2	Muscle	SZ-208	7.250	7.344	1.30
3	Soft tissue	SZ-207	7.010	7.054	0.63
4	Compact bone	BE-T	13.179	13.386	1.57
5	Cortical bone	BE-H	11.697	12.005	2.63
6	Inner bone	BE-N	9.141	9.311	1.86
7	Muscle + adipose	SZ-220	7.130	7.163	0.46
8	Cartilage bone	SZ-160	7.350	7.919	7.74

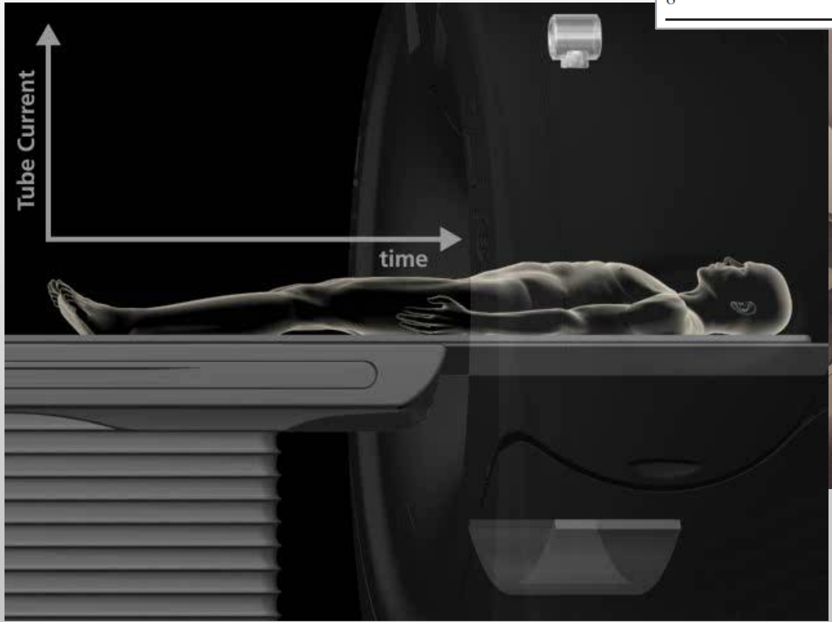

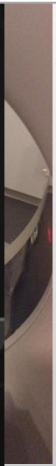

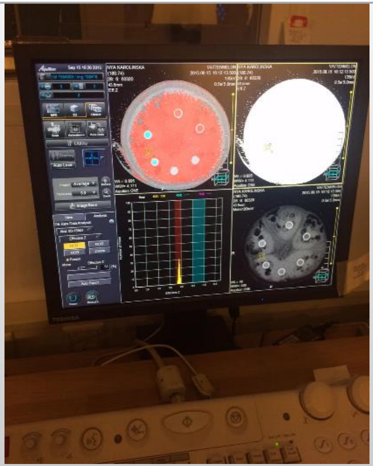

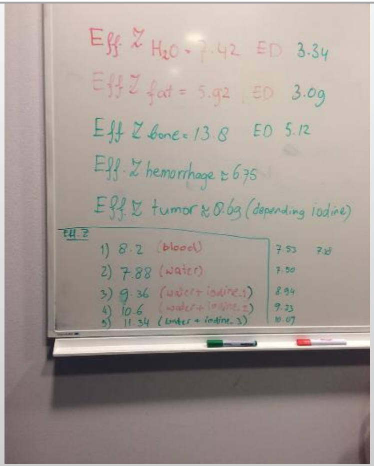

Source: Fuminari et al, DE analysis at 320-detector CT (2014)

Publication

1. Chaytor R.J. et al, "*Determining the composition of urinary tract calculi using stone-targeted dual-energy CT: evaluation of a low-dose scanning protocol in a clinical environment*", Br J Radiology, (2016)

2. Fuchs M. et al, "*Acute vertebral fracture after spinal fusion: a case report illustrating the added value of single-source dual- energy CT to MRI in a patient with spinal instrumentation*", Skeletal Radiology, (2016)

3. Kiefer T. et al, "*Single source dual-energy CT in the diagnosis of gout: Diagnostic reliability in comparison to digital radiography and conventional computed tomography of the feet*", Eur J of Radiology 85 (2016)

4. Funabashi N. et al, "*Influence of tube voltage and heart rate on Agatson Ca score, novel ECG-gated dual energy reconstruction 320 slice CT technique*", Int. J. of Cardiology, Vol. 180, (2015)

5. Diekhoff T. et al, "*First experience with single-source dual-energy computed tomography in six patients with acute arthralgia : a feasibility experiment using joint aspiration as a reference*", Skeletal Radiology, (2015)

6. Fuminari T. et al, "*Measurement of Electron Density & Effective Atomic Number by Dual-Energy Scan Using a 320-Detector CT Scanner with Raw Data-Based Analysis: A Phantom Study*", J of comp assisted tomography, (2014)

7. Cai X. et al, "*Impact of reduced-radiation dual-energy protocols using 320-detector row computed tomography for analyzing urinary calculus components: initial in vitro evaluation*", Urology, Vol. 84, (2014)

8. Diekhoff T. et al, "*Detection and Characterization of Crystal Suspensions Using Single-Source Dual Energy Computed Tomography: A Model of Crystal Arthropathies*", Investigative Radiology, (2014)

9. Tatsugami F. et al, "*Dual energy raw data based decomposition analysis on Aquilion ONE*", VISIONS 23, (2014)
10. Buckley O. et al, "*Dual energy CT in the Prime time*", VISIONS 23, (2014)
11. Rogalla P. et al, "*One Man's Trash is Another Man's Treasure: Dual-energy in Bowel Ischemia*", ISCT (2015)

“il futuro già attualità”

TOSHIBA Super High resolution CT

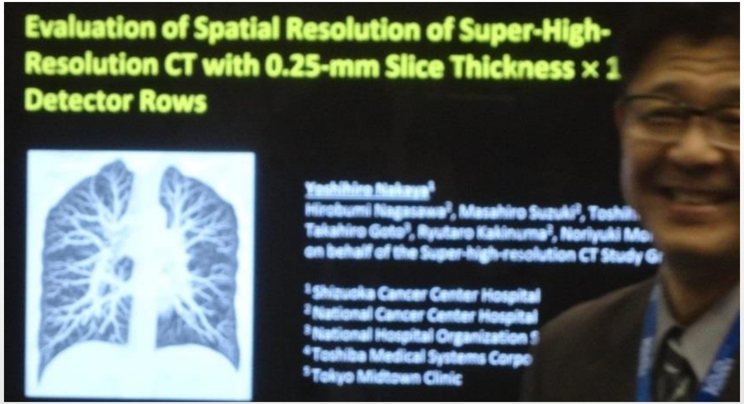

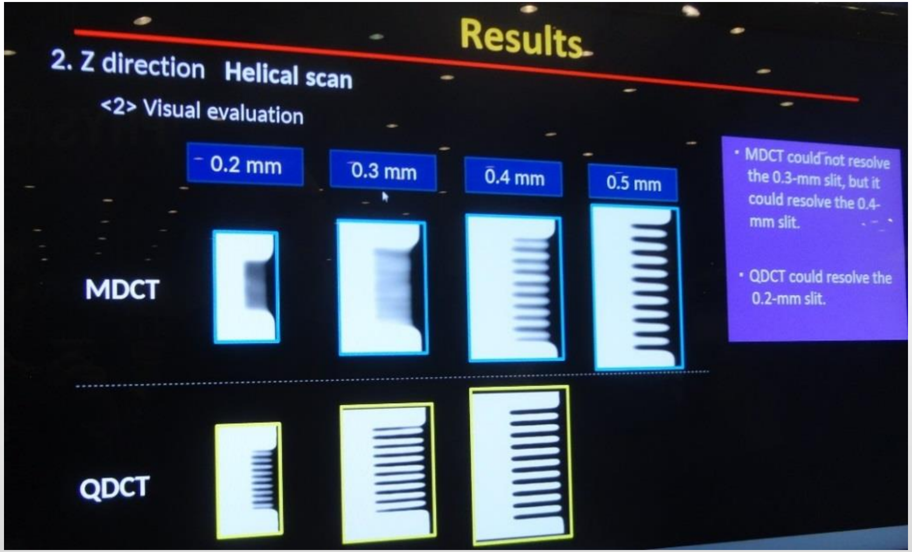

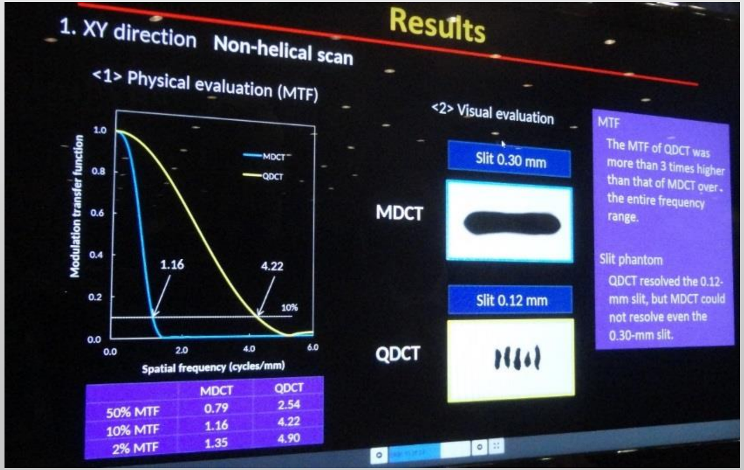

Note:

With super high resolution CT, MTF @10% is approx 4x as high as current system (see Figure left).

This can be seen in evaluation of lp/cm images (see Figure above).

TOSHIBA Super High resolution CT

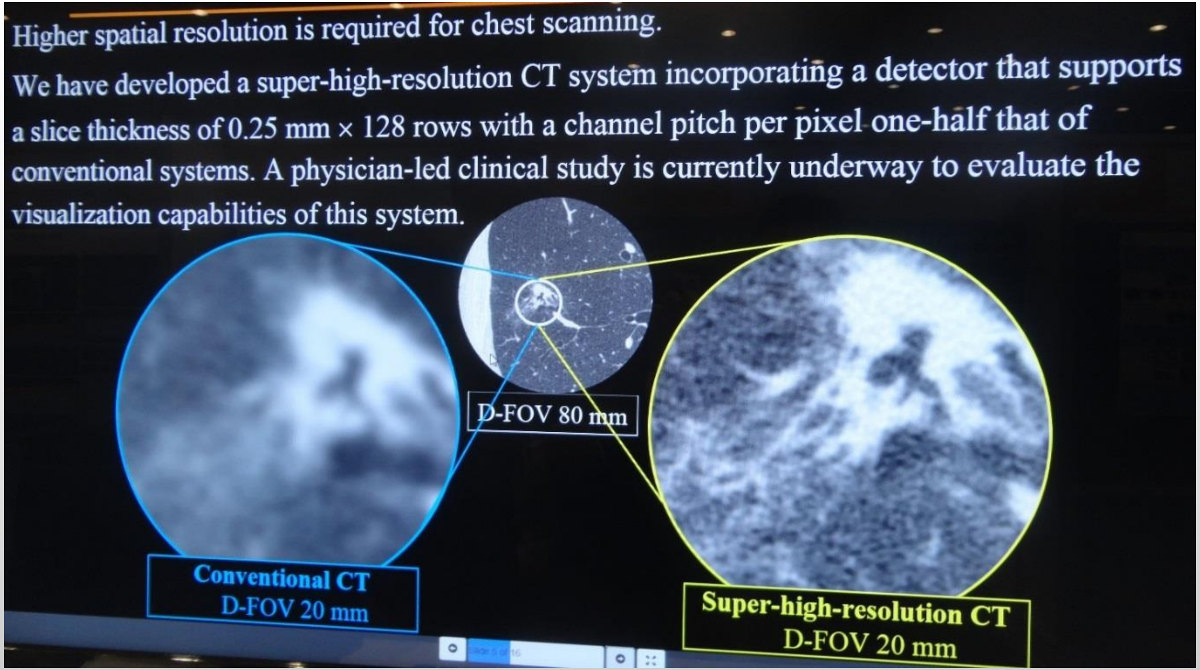

<u>Note:</u>

Clinical images show the difference between conventional CT and super high resolution CT @ D-FOV of 20mm. The latter (right image) shows much more details and clinical values compared to the former (left image).

al di là dei "numeri"

Computer

Gantry

Spessore dello strato

Generatore

Lettino

Tubo Radiogeno

- Il numero degli strati rappresenta il parametro di riferimento per la suddivisione in classi merceologiche/economiche

- Si parla di «Riduzione della Dose»

- Si elencano una serie di programmi applicativi che devono essere inseriti

Ma si valutano sempre gli stessi parametri !

Classificazione Nazionale Dispositivi

Z11030601	TOMOGRAFI ASSIALI COMPUTERIZZATI - INFERIORE O UGUALE A 2 STRATI
Z11030602	TOMOGRAFI ASSIALI COMPUTERIZZATI - SUPERIORE A 2 STRATI ED INFERIORE A 16 STRATI
Z11030603	TOMOGRAFI ASSIALI COMPUTERIZZATI - SUPERIORE O UGUALE A 16 STRATI ED INFERIORE A 64 STRATI
Z11030605	TOMOGRAFI ASSIALI COMPUTERIZZATI - SUPERIORE O UGUALE A 64 STRATI ED INFERIORE A 128 STRATI
Z11030606	TOMOGRAFI ASSIALI COMPUTERIZZATI - SUPERIORE O UGUALE A 128 STRATI ED INFERIORE A 256 STRATI
Z11030607	TOMOGRAFI ASSIALI COMPUTERIZZATI - SUPERIORE O UGUALE A 256 STRATI
Z11030680	TOMOGRAFI ASSIALI COMPUTERIZZATI (TAC, TC) - COMPONENTI ACCESSORI HARDWARE
Z11030682	TOMOGRAFI ASSIALI COMPUTERIZZATI (TAC, TC) - COMPONENTI ACCESSORI SOFTWARE
Z11030685	TOMOGRAFI ASSIALI COMPUTERIZZATI (TAC, TC) - MATERIALI SPECIFICI
Z11030699	TOMOGRAFI ASSIALI COMPUTERIZZATI (TAC, TC) NON ALTRIMENTI CLASSIFICATI

Comparazione tra TC a 80 e 160 strati

	80 strati	160 strati
Numero di file detettori asse Z	80	80
Numero detettori/fila	896	896
Spessore minimo dello strato	0,5 mm	0, 5 mm
Larghezza detettore asse Z	40 mm	40 mm
Volume acquisito in 10 sec. Pitch 1	1142,8 mm	1142,8 mm
Risoluzione longitudinale in spirale	0,31 mm	0,31 mm
Risoluzione longitudinale in assiale (volume)	0,35 mm	0,31 mm

La contestualizzazione dei numeri

Risoluzione di contrasto	4 mm @ 0,3%	kV	120	mAs	250	Dose mGy	27	kW	30	Concorrente X	305%
Risoluzione di contrasto	4 mm @ 0,3%	kV	120	mAs	82	Dose mGy	8,4	kW	9,84	Toshiba (Prime)	
Risoluzione di contrasto	2 mm @ 0,32%	kV	120	mAs	353	Dose mGy	31,1	kW	42,36	Concorrente X	186%
Risoluzione di contrasto	2 mm @ 0,3%	kV	120	mAs	190	Dose mGy	18,6	kW	22,8	Toshiba (Prime)	

Risoluzione di contrasto	4 mm @ 0,3%	kV	120	mAs	250	max mA a 0,3 sec.	833,33 mA	100 kW	Concorrente X
Risoluzione di contrasto	4 mm @ 0,3%	kV	120	mAs	82	max mA a 0,3 sec.	273,33 mA	33 kW	Toshiba (Prime)
Risoluzione di contrasto	2 mm @ 0,32%	kV	120	mAs	353	max mA a 0,3 sec.	1176,66 mA	142 kW	Concorrente X
Risoluzione di contrasto	2 mm @ 0,3%	kV	120	mAs	190	max mA a 0,3 sec.	633,33 mA	76 kW	Toshiba (Prime)

Grazie

Made For *life*